Molecular Pharmacology Fast Forward. Published on August 23, 2016 as DOI: 10.1124/mol.116.104521
This article has not been copyedited and formatted. The final version may differ from this version.

Protein RS1 (*RSC1A1*) Downregulates the Exocytotic Pathway of Glucose Transporter SGLT1 at Low Intracellular Glucose via Inhibition of Ornithine Decarboxylase

Chakravarthi Chintalapati, Thorsten Keller, Thomas D. Mueller, Valentin Gorboulev, Nadine Schäfer, Ilona Zilkowski, Maike Veyhl-Wichmann, Dietmar Geiger, Jürgen Groll, Hermann Koepsell

Institute of Anatomy and Cell Biology, University of Würzburg, 97070 Würzburg, Germany (C.C., V.G., M.V., H.K.); Department of Molecular Plant Physiology and Biophysics, Julius-von-Sachs-Institute, University of Würzburg, 97082 Würzburg, Germany (T.K., T.D.M., N.S., D.G., H.K.); Department of Functional Materials in Medicine and Dentistry, University Hospital Würzburg, Germany (J.G., I.Z.)

Molecular Pharmacology Fast Forward. Published on August 23, 2016 as DOI: 10.1124/mol.116.104521
This article has not been copyedited and formatted. The final version may differ from this version.

Running title: Short-term Regulation of SGLT1 by RS1 via Inhibition of ODC

Corresponding author: Hermann Koepsell, Department of Molecular Plant Physiology and Biophysics, Julius-von-Sachs-Institute, Julius-von-Sachs-Platz 2, 97082 Würzburg, Germany, phone +49 931 3182700; fax +49 931 31-82087; E-mail: Hermann@Koepsell.de

Number of text pages: 26

Number of tables: 1

Number of figures: 10

Number of references: 50

Number of words in the abstract: 249

Number of words in the introduction: 593

Number of words in the discussion: 1465

ABBREVIATIONS: AMG, α-methyl-D-glucopyranoside; AZ, antizyme; AZIN, antizyme inhibitor; BFA, brefeldin A; BBM, brush-border membrane; BTXB, botulinumtoxin B; CNT1, concentrative nucleoside transporter 1; DMEM, Dulbecco´s modified Eagle medium; DFMO, difluoromethyl-ornithine; DTT, dithiothreitol; EC_{50}, half maximal effective concentration; EDC, 1-Ethyl-3-(3-di-methylaminopropyl)-carbodiimide; GFP, green fluorescent protein; GLUT2, glucose transporter 2; GLUT4, glucose transporter 4; GST, glutathione-S-transferase; IPTG, isopropyl-1-thio-β-D-galactopyranoside; IC_{50}, half maximal concentration for inhibition; K_D, equilibrium binding dissociation constant; k_{off}, dissociation rate constant; k_{on}, association rate constant; M_r, relative molecular mass; NHS, sulfo-N-hydroxysuccinimide; ODC ornithine decarboxylase; PBS, phosphate buffered saline; RS1, product of gene *RSC1A1*; RS1-Reg, NH2-terminal regulatory domain of RS1; RU, resonance unit; SGLT1, Na^+-D-glucose cotransporter 1; SPR, surface plasmon resonance; TGN, *trans*-Golgi network; YFP, yellow fluorescent protein.

Molecular Pharmacology Fast Forward. Published on August 23, 2016 as DOI: 10.1124/mol.116.104521
This article has not been copyedited and formatted. The final version may differ from this version.

ABSTRACT

Na^+-D-glucose cotransporter SGLT1 is rate-limiting for glucose absorption in small intestine. Shortly after intake of glucose-rich food SGLT1 abundance in the luminal membrane of small intestine is increased. This upregulation occurs via glucose-induced acceleration of the release of SGLT1-containing vesicles from *trans*-Golgi network (TGN) which is regulated by a domain of protein RS1 (*RSC1A1*) named RS1-Reg. Dependent on phosphorylation RS1-Reg blocks release of vesicles containing SGLT1 or the concentrative nucleoside transporter CNT1. The hypothesis has been raised that RS1-Reg binds to different receptor proteins at the TGN which trigger release of vesicles with different transporters. To identify the presumed receptor proteins two-hybrid screening was performed. Interaction with ornithine decarboxylase ODC1, the rate-limiting enzyme of polyamine synthesis, was observed and verified by immunoprecipitation. Binding of RS1-Reg mutants to ODC1 was characterized using surface plasmon resonance. Inhibition of ODC1 activity by RS1-Reg mutants and the ODC1 inhibitor difluoromethyl-ornithine (DFMO) was measured in absence and presence of glucose. In addition, short-term effects of DFMO, RS1-Reg mutants, the ODC1 product putrescine and/or glucose on SGLT1 expressed in oocytes of *Xenopus laevis* were investigated. High affinity binding of RS1-Reg to ODC1 was demonstrated and evidence for a glucose binding site in ODC1 was provided. Binding of RS1-Reg to ODC1 inhibits the enzymatic activity at low intracellular glucose which is blunted at high intracellular glucose. The data suggest that generation of putrescine by ODC1 at the TGN stimulates release of SGLT1-containing vesicles. This indicates a biomedical important role of ODC1 in regulation of glucose homeostasis.

Molecular Pharmacology Fast Forward. Published on August 23, 2016 as DOI: 10.1124/mol.116.104521
This article has not been copyedited and formatted. The final version may differ from this version.

Introduction

For rapid adaption of cellular uptake to physiological demands the concentrations of transporters in the plasma membrane can be changed by regulation of endocytosis and/or exocytosis of transporter-containing vesicles. Endocytotic vesicles are delivered to endosomes where they are sorted for degradation or recycling to the plasma membrane. Transporter-containing vesicles delivered to the plasma membrane may be also derived from the Golgi as has been described for upregulation of Na^+-D-glucose cotransporter SGLT1 in small intestine after uptake of glucose-rich food (Gorboulev et al., 2012; Veyhl-Wichmann et al., 2016). The increased concentration of intracellular glucose in the enterocytes activates the release of SGLT1-containing vesicles from the Golgi (Veyhl et al., 2003, 2006; Kroiss et al., 2006; Veyhl-Wichmann et al., 2016). Due to rapid turnover of SGLT1 in the plasma membrane including endocytosis and degradation (Wright et al., 1997) glucose-dependent release of SGLT1-containing vesicles from the Golgi may lead to a 2-4fold upregulation of SGLT1 in the BBM within minutes (Veyhl-Wichmann et al., 2016).

The intracellular 67-68 kDa protein RS1 (gene *RSC1A1*) is critically involved in glucose-dependent posttranslational regulation of SGLT1 at the Golgi. RS1 is encoded by a single copy gene that first emerged in mammals (Veyhl et al., 1993; Lambotte et al., 1996; Reinhardt et al., 1999; Osswald et al., 2005). In LLC-PK1 cells RS1 was detected at the *trans*-Golgi network (TGN) where it was colocalized with SGLT1 and dynamin (Kroiss et al., 2006). When studying the effects of RS1 on mammalian transporters expressed in oocytes of *Xenopus laevis* posttranslational regulation of Na^+-D-glucose cotransporters, Na^+-nucleoside cotransporters and organic cation transporters was observed (Reinhardt et al., 1999; Veyhl et al., 2003; Errasti-Murugarren et al., 2012). We analysed posttranslational regulation of human SGLT1 (hSGLT1) and human Na^+-nucleoside cotransporter CNT1 (hCNT1) by expressing the transporters in oocytes and measuring short-term effects of injected hRS1-fragments on transport activities and transporter concentrations in the plasma membrane (Veyhl et al., 2003, 2006; Vernaleken et al., 2007; Errasti-Murugarren et al., 2012). We observed that downregulation of hSGLT1 and hCNTs by hRS1 and/or hRS1 fragments was prevented when the Golgi was dissociated with brefeldin A (BFA) or fusion of exocytotic vesicles with the plasma

Molecular Pharmacology Fast Forward. Published on August 23, 2016 as DOI: 10.1124/mol.116.104521
This article has not been copyedited and formatted. The final version may differ from this version.

membrane was blocked with botulinumtoxin B (BTXB) but was not changed by blockers of endocytosis. We therefore concluded that RS1 blocks the exocytotic release of the transporters from the TGN. Recently we showed that posttranslational regulation of hSGLT1 and hCNT1 are mediated by an N-terminal domain of human RS1 (hRS1) termed hRS1-Reg, which contains many predicted phosphorylation sites of protein kinases (Veyhl-Wichmann et al., 2016). Since it was observed that hRS1-Reg downregulates hSGLT1 expression in a glucose-dependent manner whereas downregulation of hCNT1 expression is independent of glucose, and because the efficacy of hRS1-Reg for downregulation of hSGLT1 versus hCNT1 was differentially dependent on phosphorylation of hRS1-Reg, we concluded that hRS1-Reg downregulates different exocytotic transporter pathways. We raised the hypothesis that differentially phosphorylated forms of hRS1-Reg bind to different receptor proteins at the TGN that are involved in regulation of different exocytotic pathways for plasma membrane transporters. Evidence was provided that short-term upregulation of SGLT1 in small intestine is due to a glucose-induced blunting of RS1-Reg-mediated blockage of the exocytotic pathway of SGLT1 (Veyhl-Wichmann et al., 2016).

The aim of the present study was to identify one of the hypothesized receptor proteins of hRS1-Reg. We performed two-hybrid screening with an N-terminal domain of hRS1 and characterized one of the identified interacting proteins, the human ornithine decarboxylase 1 (hODC1). Here we present evidence that hODC1 is a receptor protein for hRS1-Reg that is involved in glucose-dependent short-term regulation of hSGLT1.

Materials and Methods

Materials. α-Methyl-D[^{14}C]glucopyranoside ([^{14}C]AMG) (11.1 GBq/mmol) and [5-^{3}H]uridine (0.91 TBq/mmol) were obtained from American Labeled Chemical Inc. (St. Louis, MO) and D,L-[1-^{14}C]ornithine (2.07 TBq/mmol) was purchased from Hartmann Analytic (Braunschweig, Germany). S-protein agarose (agarose beads with coupled S-protein) was purchased from Merck (Darmstadt, Germany) and glutathione-sepharose 4B beads from GE-Healthcare (Munich, Germany). DL-α-difluoromethylornithine (DFMO), bovine thrombin, Accutase® solution, anti c-myc agarose (agarose

Molecular Pharmacology Fast Forward. Published on August 23, 2016 as DOI: 10.1124/mol.116.104521
This article has not been copyedited and formatted. The final version may differ from this version.

beads with linked anti-myc antibodies), and anti mouse IgG-agarose beads (agarose beads with covalently linked antibodies against mouse IgG raised in goat) (A6531) were obtained from Sigma-Aldrich (Taufkirchen, Germany). Protease inhibitor cocktail set III was provided by Calbiochem (Darmstadt, Germany) and prestained weight markers (BenchMark) from Life Technologies (Karlsruhe, Germany). A human cDNA library from embryonic kidney cells expressed in vector pPR3-N was obtained from Dualsystems Biotech (Schlieren, Switzerland). Bait vector pMetYCgate for the split ubiquitin assay, the linkers B1 and B2 as well as yeast strain THY.AP4 were provided by C. Ciarimboli (Brast et al., 2012). Expression vector pcDNA3 encoding for full-length human ODC fused to a C-terminal myc tag was supplied by S. Matsuzawa (Matsuzawa et al., 2005). ProteOn GLC sensor chip, 1-ethyl-3-(3-dimethylaminopropyl)-carbodiimide (EDC), sulfo-N-hydroxysuccinimide (NHS) and ethanolamine were purchased from BioRad (München, Germany), and LC-NHS-biotin from Fisher Scientific GmbH (Schwerte, Germany). Other reagents were purchased as described (Keller et al., 2005; Veyhl-Wichmann et al., 2016, Vernaleken et al., 2007).

Antibodies. Mouse monoclonal antibody against myc (anti-myc-Ab) (OP10) was obtained from Calbiochem (Darmstadt, Germany) and mouse monoclonal antibody against GFP (anti-GFP-Ab) (MMS-118P) from Covance (Freiburg, Germany). An antibody against hODC1 raised in mouse (anti-hODC1-Ab) was purchased via Antibodies-online (ABIN518505). Polyclonal antibodies against full-length hRS1 (anti-hRS1-Ab) containing an N-terminal S-tag and a C-terminal His-Tag (S-hRS1-H) were raised in rabbits. Cloning and purification of S-hRS1-H is described below. Polyclonal immune serum against a peptide within hRS1-Reg (amino acids 40-57 of hRS1) containing a C-terminal cysteine (IKPSDSDRIEPKAVKALK-C) was raised in rabbits (anti-hRS1-Reg-P-Ab). The antibody was purified employing antigenic peptide coupled via the C-terminal cysteine to polyacrylamide particles.

Cloning. To clone the bait for the split ubiquitin analysis we used hRS1 (Lambotte et al., 1996) as template. An N-terminal hRS1 fragment comprising amino acids 1-312 with linkers termed B1 and B2 for insertion into the bait vector pMetYCgate (Obrdlik et al., 2004) was amplified by PCR. A forward primer with B1 linker (underlined) 5´-<u>ACA AGT TTG TAC AAA AAA GCA GGC TCT</u> CCA ACC

Molecular Pharmacology Fast Forward. Published on August 23, 2016 as DOI: 10.1124/mol.116.104521
This article has not been copyedited and formatted. The final version may differ from this version.

ACC ATG TCA TCA TTA CCA ACT TCA GAT GGG-3′ and a reverse primer with B2 linker (underlined) 5′- TCC GCC ACC ACC CAC TTT GTA CAA GAA AGC TGG GTA GGG CTG TAA ATC CTG AGT GGA AAT GG-3′ were used. The amplified constructs were cloned into the pMetYCgate vector (Obrdlik et al., 2004) using the PstI and HindIII restriction sites. The constructs were expressed in yeast strain THY.AP4 (Obrdlik et al., 2004).

For immunoprecipitation hRS1 fragments expressed in pEGFP-TEV-S-Tag vector (Filatova et al., 2009) were used and constructs were generated in which green fluorescent protein (GFP) followed by an S-Tag was linked to the N-terminus of hRS1(2-312) (GFP-S-hRS1(2-312) or hRS1(2-98) (GFP-S-hRS1(2-98)). To clone GFP-S-hRS1(2-312) and GFP-S-hRS1(2-98) RS1 fragments framed with linkers containing restriction sites were prepared by PCR. In case of hRS1(2-312) the forward primer 5'-GCCTGCAGGGATCCTGTCATCATTACCAACTTCAG-3' contained a PstI recognition site (underlined) and the reverse primer 5'-GCGGTACCTCGAGTCAGGGCTGTAAATCCTGAGTG-3' contained an Acc65I recognition site (underlined). hRS1was used as template for the PCR. Employing the PstI and Acc65I restriction sites the PCR product was inserted into vector pEGFP-TEV-S-Tag using the open reading frame of GFP and the S-Tag. For PCR amplification of the hRS1(2-98) fragment with linkers GFP-S-hRS1(2-312) was used as template. The forward primer 5'-CTCTCGGCATGGACGAGC-3' located C-terminal of the GFP coding region and the reverse primer 5'-GCGGTACCTCACTGCATAGGCATAGCTGG-3' containing a Acc65I recognition site (underlined) were used. The PCR product was inserted into the vector pEGFP-TEV-S-Tag using the PstI and Acc65I restriction sites.

For functional characterization of purified hRS1-Reg peptides containing the amino acids 16-98 of hRS1, hRS1-Reg(S20A) and hRS1-Reg(S20E), previously described constructs in vector pET21a were used, which encode the peptides with an N-terminal cysteine (Veyhl-Wichmann et al., 2016). Under the reducing conditions in the cytosol and in the presence of DTT (Fig. 3B) dimerization of these peptides by formation of intermolecular disulfide is prevented. Using hRS1 (Lambotte et al., 1996) we first amplified a construct containing hRS1-Reg with an additional N-terminal cysteine residue in vector pET21a (Novagen, Darmstadt, Germany). hRS1-Reg was cloned in the open reading

Molecular Pharmacology Fast Forward. Published on August 23, 2016 as DOI: 10.1124/mol.116.104521
This article has not been copyedited and formatted. The final version may differ from this version.

frame with the C-terminal His-tag encoded in pET21a. The mutations S20A and S20E were introduced in the construct by applying the PCR overlap extension method (Veyhl-Wichmann et al., 2016).

As control peptide for interaction analysis using surface plasmon resonance (SPR) we cloned a peptide containing the amino acids 150-312 of hRS1. For PCR amplification vector pET21a containing hRS1 (hRS1/pET21a) was used as template. A forward primer with a Bgl II site and a reverse primer with an Xho I site were used. The PCR product was digested with Bgl II and Xho I and cloned into pET21a vector cut with Bg1 II and Xho I.

For overexpression of human ODC1 (hODC1) in *E.coli* and purification on glutathione-sepharose 4B the sequence encoding for hODC1 was obtained by PCR using hODC1 in pcDNA3 plasmid (Matsuzawa et al., 2005) as template. A forward primer with an Acc 65I recognition site and a reverse primer with an Xho I site were used. The PCR product was cut with Acc 65I and Xho I and ligated to the pET42b vector which was treated with the same restriction enzymes. The resulting construct was transformed into the *E. coli* strain BL21(DE3)Star (Invitrogen) for protein expression. The expression yields a fusion protein consisting of glutathione-S-transferase (GST) followed by a His-tag, a thrombin cleavage site, the S-tag, hODC1 protein, and a second His-tag (hODC1/pET42b).

Full-length hRS1 was expressed in Sf9 insect cells. Therefore hRS1 containing an N-terminal S-tag and a C-terminal His-Tag (S-hRS1-H) was cloned into vector pVL1392 (BD Biosciences, Erembodegem, Belgium) as described (see S-tag-hRS1-His/pVL1392 in (Veyhl et al. 2006)).

For expression of human ODC1 (hODC1) in oocytes the hODC1 coding sequence was cloned into vector pRSSP (Busch et al., 1996) using Eco RI as 5´ and Xho I as 3´ restriction sites of the vector (hODC1/pRSSP).

To visualize localization of hSGLT1 in oocytes yellow fluorescence protein (YFP) was fused to the C-terminus of hSGLT1 (hSGLT1-YFP). Therefore the complementary DNA of hSGLT1 was cloned into an YFP containing oocyte expression vector (see vector pNB1uYFP in (Nour-Eldin et al., 2006)) using an advanced uracil-excision-based cloning technique (Nour-Eldin et al., 2006).

Molecular Pharmacology Fast Forward. Published on August 23, 2016 as DOI: 10.1124/mol.116.104521
This article has not been copyedited and formatted. The final version may differ from this version.

Two-Hybrid Screening by the Split Ubiquitin Assay. To identify proteins that interact with RS1 at the Golgi we used the two-hybrid split ubiquitin assay which has been developed to identify proteins that interact with membrane proteins (Brast et al., 2012). The yeast reporter THY.AP4 strains transfected with empty pMetYCgate vector or pMetYCgate containing hRS1(1-312) were cotransformed with a human cDNA library in vector pPR3-N. Colonies reacting positive in the β-galactosidase assay were selected on synthetic complete medium lacking leucine, tryptophane, histidine and uracil. Plasmid DNAs from positive colonies were isolated, transformed into *E.coli* DH10B (Grant et al., 1990) and amplified. DNA sequences were determined after PCR amplification using the primer 5'-GTC GAA AAT TCA AGA CAA GG-3'.

Expression and Purification of hODC1 and hRS1. hODC1 was expressed in E. coli. *E. coli* strain BL21(DE3)Star (Live Technologies, Darmstadt, Germany) harboring the pET42b plasmid encoding a GST-hODC1 fusion protein with a thrombin site between the N-terminal GST-tag and hODC1 was cultivated at 23°C until a density of OD_{600} = 0.6 – 0.8 was obtained. After induction of protein expression with 0.2 mM isopropyl-1-thio-β-D-galactopyranoside (IPTG), bacteria were grown for 24 h. Thereafter bacteria were pelleted by 15 min centrifugation at 6,000 × g, washed, and resuspended in 20 mM Tris, pH 8.3, 150 mM NaCl, 10 mM EDTA, 2 mM DTT, 1 mM PMSF. For lysis bacteria were sonified at 4^{o} C, and cellular debris was sedimented by ultracentrifugation for 1 h at 100,000 × g. Protein purification was performed by adding 0.5 ml of glutathione-sepharose 4B beads to 20 ml lysate and incubating the suspension for 1 h at 4^{o}C. The affinity resin was pelleted by centrifugation for 5 min at 500 × g, washed with 20 mM Tris, pH 8.3, 150 mM NaCl, 2 mM DTT and incubated in 1 ml washing buffer supplemented with bovine thrombin (2 units) for 2 h at 37°C to release hODC1. After centrifugation for 5 min at 500 × g, purified hODC1 was obtained in the supernatant and dialyzed against 10 mM HEPES pH 7.5, 150 mM NaCl, pH7.5, 0.005% (v/v) Tween 20 (for SPR-measurements) or against 50 mM Tris-HCl, pH 7.2 (for assays of ODC activity). The purification was monitored using SDS PAGE and Coomassie staining (Fig. 3A).

Tagged full-length hRS1 protein (S-hRS1-H) was expressed in Sf9 insect cells using vector S-tag-hRS1-His/pVL1392 and purified on Ni^{2+}-NTA-agarose as described (Veyhl et al. 2006).

Molecular Pharmacology Fast Forward. Published on August 23, 2016 as DOI: 10.1124/mol.116.104521
This article has not been copyedited and formatted. The final version may differ from this version.

Expression and Purification of hRS1-Reg, hRS1-Reg Variants and hRS1(150-312). *E. coli* bacteria (strain BL21 Star) were transformed with pET21a plasmids containing His-tagged hRS1-Reg, hRS1-Reg mutants or hRS1(150-312). Protein expression was induced by adding 1 mM IPTG and bacteria were subsequently grown for 3 h at 30°C. After 15 min centrifugation at 6,000 × g, bacteria were washed, suspended in 20 mM Tris-HCl pH 8.0 containing 500 mM NaCl and 50 mM imidazole. The cells were lysed by sonication at 4°C, and cellular debris was removed by 1 h centrifugation at 100,000 × g. For protein purification the supernatants were mixed with Ni^{2+}-NTA-agarose and the beads were incubated for 1 h under rotation and poured into an empty gravity flow column. After washing with 20 mM Tris pH 8.0 containing 500 mM NaCl and 50 mM imidazole, protein was eluted with 20 mM Tris pH 8.0 containing 500 mM NaCl and 500 mM imidazole. Fractions containing purified protein were pooled and dialyzed against 10 mM HEPES pH 7.5, 150 mM NaCl, pH7.5, 0.005% (v/v) Tween 20 for SPR-measurements or against 50 mM Tris-HCl pH 7.2 for enzymatic assays.

SDS-PAGE and Western Blotting. SDS-PAGE and Western botting were performed as described (Keller et al., 2005). For SDS-PAGE, protein samples were treated for 30 min at 37°C in 60 mM Tris-HCl, pH 6.8 containing 2% (w/v) SDS and 7% (v/v) glycerol (SDS-PAGE sample buffer). With the exception of one gel in Fig. 3B, 100 mM dithiothreitol (DTT) was added to the SDS-PAGE sample buffer. The gels were stained with Coomassie brilliant blue. Separated proteins were transferred to polyvinyl difluoride membrane and stained with antibodies raised in rabbits (anti-hRS1-Ab 1:10,000, anti-hRS1-Reg-P-Ab 1:5,000, or mice (anti-myc-Ab, anti-GFP-Ab, anti-hODC1-Ab) using peroxidase-conjugated secondary antibodies against rabbit or mouse IgG, respectively. Bound secondary antibodies were visualized by enhanced chemiluminescence. For determination of apparent molecular masses (M_r) prestained weight markers were used.

Cultivation and harvesting of Caco-2 Cells. Caco-2 cells were cultivated until forming a confluent polarized monolayer as described (Kipp et al., 2003). Cells were grown for 18 days at 37°C on Petri dishes in minimal essential medium containing 1 mM D-glucose and supplemented with 10% fetal calf serum, 1% nonessential amino acids and 1% glutamine. The cells were detached using Accutase®

Molecular Pharmacology Fast Forward. Published on August 23, 2016 as DOI: 10.1124/mol.116.104521
This article has not been copyedited and formatted. The final version may differ from this version.

solution, collected by low speed centrifugation, washed with phosphate buffered saline (PBS), and suspended in ice-cold PBS containing protease inhibitor cocktail set III of Calbiochem.

Coprecipitation Experiments. For coprecipitation of overexpressed proteins, HEK293 cells were transiently transfected with vectors encoding for GFP-S, GFP-S-hRS1(2-312) or GFP-S-hRS1(2-98) and hODC1 containing a myc tag (hODC-myc). The four proteins were expressed to similar levels. After washing at 0^{o}C with PBS buffer cells were detached from culture dishes and suspended at 0^{o}C in 10 mM HEPES pH 7.2, 142 mM KCl, 5 mM $MgCl_2$, 2 mM EGTA, 0.5% (v/v) NP-40 containing 0.1 µM PMSF and 10 µl/ml of protease inhibitor cocktail from Calbiochem (lysis buffer). The suspensions were sonicated at 0^{o}C and non-soluble material was removed by 1 h centrifugation at 100,000 × g. The pull down assays with S-protein agarose beads or anti c-myc agarose beads were performed at 4^{o}C. Thirty µl of suspended agarose beads were added to 0.5 ml of the 100,000 × g supernatant which contained 0.5 mg protein. The suspension was mixed for 1 h by rotation. The beads were collected by centrifugation at 6,000 × g and washed thrice with lysis buffer. Proteins bound to the S-protein agarose beads or the anti c-myc agarose beads were released from the beads by incubation for 5 min at 95^{0}C in the presence of 1 % (w/v) SDS. The proteins were analyzed by SDS-PAGE and Western blotting.

Coprecipitation of endogenously expressed hRS1-Reg with hODC1 was performed with membranes isolated from differentiated Caco-2 cells. Caco-2 cells in PBS containing protease inhibitors were disrupted by sonication on ice, and nuclei and cell organelles were removed by centrifugation at 1000 × g and 10,000 × g, respectively. The 10,000 × g supernatant (Fig. 2A, cleared lysate) was centrifuged for 1 h at 100,000 × g (4^{o}C). The 100,000 × g supernatant (Fig. 2A, cytosol) was removed whereas the pellet (Fig. 2A, total cell membranes) was washed with PBS. After solubilization of the membranes in PBS containing 2% CHAPS (solubilization buffer) the solubilized membranes (Fig. 2B) were incubated for 1 h at room temperature with an antibody against hODC1 raised in mouse (anti-hODC1-Ab, 1:5,000). For precipitation of hODC1-protein complexes, anti mouse IgG-agarose beads were added and the suspension was incubated for 1 h at room temperature. As control, solubilization buffer containing anti-hODC1-Ab was incubated with anti mouse IgG-agarose beads. The beads were isolated by low speed centrifugation and washed with PBS. Bound proteins (Fig. 2B, Ag-eluate, Ag-

Molecular Pharmacology Fast Forward. Published on August 23, 2016 as DOI: 10.1124/mol.116.104521
This article has not been copyedited and formatted. The final version may differ from this version.

eluate control) were removed by incubation of the beads for 15 min at 95°C with SDS-PAGE sample buffer without DTT.

Interaction Analysis Using Surface Plasmon Resonance. Interactions between recombinant hODC1 and the peptides hRS1-Reg(S20E) or hRS1-Reg(S20A) were measured by surface plasmon resonance (SPR) using a ProteOn system (BioRad). Measurements were performed at 25°C using HBS150T (10 mM HEPES pH 7.4, 150 mM NaCl, 3.4 mM EDTA, 0.005% (v/v) Tween 20) as running buffer, which was freshly supplemented with 1 mM dithiothreitol (DTT) to avoid multi-merization of the RS1-Reg peptides containing free cysteine residues (Fig. 3B). For experiments determining the influence of glucose on the hODC1-hRS1-Reg interaction 1 mM D-glucose was added to the running buffer. All interaction analysis data reported in the manuscript were obtained using the so-called single-shot kinetics setup (chip rotated into the horizontal orientation), which allows to measure the five routinely used analyte concentrations and the buffer control simultaneously across six identical coated interaction spots.

For immobilization of hODC1 onto the sensor surface, the carboxylate groups of a GLC sensor chip (Biorad) were activated first by perfusing a 1:1 mixture of sulfo-N-hydroxysuccinimide (NHS) and 1-ethyl-3-(3-dimethylaminopropyl)carbodiimide (EDC) according to the manufacturer's re-commendation. Then streptavidin (40 µg ml^{-1} in 10 mM sodium acetate pH 4.0) was injected onto the activated sensor for 360 s at a flow rate of 30 µl × min^{-1} to result in streptavidin coating to a final density of 2000 to 2100 resonance units (RU). Unreacted activated carboxylate groups were quenched by injecting 1 M ethanolamine pH 8.5 for 300 s. Purified recombinant hODC1 was biotinylated using LC-NHS-biotin in a molar ratio of 2:1 and unreacted biotin was removed by dialysis against PBS. The biotinylated hODC1 protein was then injected at a concentration 5-10 µg ml^{-1} in running buffer and perfused over the streptavidin-coated sensor until a coating density of 600 to 800 RU was obtained. A flow channel carrying no hODC1 as ligand was used as control to monitor interaction specificity. Interaction of the analyte to this control surface was subtracted from the raw data to allow the removal of unspecific binding and bulk face effects. Alternatively, in the single-shot kinetics setup the so-called interspots, which do not carry the immobilized ligand, were used for subtraction. RS1-

Molecular Pharmacology Fast Forward. Published on August 23, 2016 as DOI: 10.1124/mol.116.104521
This article has not been copyedited and formatted. The final version may differ from this version.

Reg(S20A) and RS1-Reg(S20E) peptides were used as analytes at five concentrations ranging from 156 to 5,000 nM. The flow rate for the acquisition of interaction data was set to 75 µl min^{-1} in all experiments. Association was measured for 120 s, then dissociation was initiated by perfusing running buffer and the dissociation phase was also monitored for 120 s. Regeneration of the chip surface was performed by injecting two 60 s pulses of 100 mM glycine pH 2.5 and 10 mM glycine pH 1.5 at a flow rate of 100 µl min^{-1}. To test the effect of the irreversible ODC inhibitor DMFO, one of two flow channels carrying hODC1 as ligand was perfused with running buffer containing 1 mM DMFO in vertical direction for at least 45 min. This approach leaves one flow channel unmodified, whereas hODC1 on the other flow channel was irreversibly modified. Then interaction of hRS1-Reg mutants with reacted and non-reacted hODC1 was analyzed in the single shot kinetics setup allowing the measurement of peptide binding to modified and non-modified hODC1 simultaneously. Interaction data were analyzed using the software ProteOn Manager version 3.1 applying a simple Langmuir type 1:1 interaction model and using global fitting for the rate constants. Association rate constant k_{on} values and dissociation rates constant k_{off} values were obtained by fitting data of individual experiments. Equilibrium binding K_D values were deduced using the equation $K_D = k_{off} / k_{on}$. All SPR experiments were performed in at least three independent experiments.

Preparation of Lipid-depleted Oocyte Homogenates. Thirty oozytes were suspendend in 200 µl of 20 mM Tris-HCl pH 7.5 containing 10 mM EDTA and protease inhibitors and homogenized using a 200 µl pipette. To remove lipids and egg yolk the homogenized material was centrifuged for 15 min at 1,000 × g (4°C). After centrifugation three phases were formed: an upper phase mainly containing lipids, a middle phase mainly containing cytosolic material, and a lower phase mainly containing egg yolk. The middle phase was removed, diluted with 20 mM Tris-HCl pH 7.5, 10 mM EDTA and centrifuged 15 min at 1,000 × g. After this centrifugation, again the middle phase was removed, diluted and centrifuged at 1,000 × g. The middle phase obtained from this third centrifugation (called lipid-depleted homogenates) was used for determination of endogenous ODC activity.

Measurement of Enzymatic Activity of Ornithine Decarboxylase. ODC activity was determined by measuring the amount of $^{14}CO_2$ liberated from L-[1-^{14}C]ornithine as described (Milovic et al.,

Molecular Pharmacology Fast Forward. Published on August 23, 2016 as DOI: 10.1124/mol.116.104521
This article has not been copyedited and formatted. The final version may differ from this version.

1998). The reaction was performed in closed reaction containers containing a needle with pierced filterpapers inside the lid. The filter papers were soaked with 20 µl of 1 M benzethonium hydroxide solution. 100 µl of 50 mM Tris-HCl pH 7.2, containing 0.7 µM pyridoxal-5-phosphate and 10 ng purified hODC1 or different amounts of lipid-depleted oocyte homogenate plus different concentrations of hRS1-Reg(S20A), hRS1-Reg(S20E), DFMO, and/or D-glucose were added to the bottom of the reaction container. To start the reaction 16 µl of 50 mM Tris–HCl pH 7.2 containing L-ornithine traced with ^{14}C-labelled L-ornithine, 2.5 mM DTT, and 0.1 mM EGTA was added and the container was closed. After 1 h incubation at 37°C the reaction was stopped by adding of 200 µl of 0.6 N perchloric acid. After 30 min incubation at 37°C the filter papers of the reaction containers were transferred into scintillation vials containing 3 ml Lumasafe scintillation cocktail (Luma LSC, Netherlands, Groningen) plus 75 µl 10% (v/v) acetic acid.

cRNA Synthesis. For cRNA synthesis human SGLT1 (hSGLT1) in vector pBSII SK (Vernaleken et al., 2007), human CNT1 (hCNT1) in vector pBSII KS (Errasti-Murugarren et al., 2012), human ODC1 (hODC1) in vector pRSSP, and hSGLT1-YFP in vector pNBI 22 were used. To prepare sense cRNAs the purified plasmids were linearized with EcoRI (hSGLT1), XbaI (hCNT1), Mlu I (hODC1) or Nhel (hSGLT1-YFP). m^7G(5′)G-capped sense cRNAs were synthesized using T3 polymerase (hSGLT1, hCNT1), T7 polymerase (hSGLT1-YFP) or SP6 polymerase (hODC1). cRNAs were prepared employing the "mMESSAGE mMachine" kit (Ambion Life Technologies) using sodium acetate precipitation. The concentrations of the cRNAs were estimated as described (Vernaleken et al. 2007).

Expression of hSGLT1, hSGLT1-YFP, hCNT1, and hODC1 and in Oocytes of *Xenopus Laevis*. Mature female *Xenopus laevis* were anesthetized by immersion in water containing 0.1% 3-aminobenzoic acid ethyl ester. After partial ovariectomy stage V or VI oocytes were treated overnight with 1 mg ml^{-1} collagenase I in Ori buffer (5 mM HEPES pH 7.6, 110 mM NaCl, 3 mM KCl, 1 mM $MgCl_2$, and 2 mM $CaCl_2$). The oocytes were washed with Ca^{2+}-free Ori buffer and kept at 16°C in modified Barth´s solution (15 mM HEPES pH 7.6, 88 mM NaCl, 1 mM KCl, 0.3 mM $Ca(NO_3)_2$, 0.4 mM $CaCl_2$, 0.8 mM $MgSO_4$) containing 12.5 µM gentamycin. Selected oocytes were injected with 50

Molecular Pharmacology Fast Forward. Published on August 23, 2016 as DOI: 10.1124/mol.116.104521
This article has not been copyedited and formatted. The final version may differ from this version.

nl of water containing cRNAs (10 ng of hSGLT1, 25 ng hSGLT1-YFP, 10 ng of hCNT1, and/or 5 ng of hODC1). For expression oocytes were incubated for two or three days at 16°C in modified Barth´s solution with gentamycin. Noninjected oocytes (tracer uptake measurements) or water-injected oocytes (electrical measurements) were incubated in parallel.

Injection of Peptides, AMG, and Biochemicals into Oocytes. Two or three days after injection of transporter cRNAs into oocytes, DFMO, putrescine, AMG, hRS1-Reg, and/or brefeldin (BFA) were injected. We injected 40 nl of K-Ori buffer containing 1.2 nmol DFMO, 0.4 pmol putrescine, 1.4 pmol hRS1-Reg, 1.25 nmol AMG, and/or 5 pmol BFA. hSGLT1-mediated uptake of [^{14}C]AMG, hCNT1-mediated uptake of [^{3}H]uridine and hSGLT1-YFP-mediated glucose-induced currents were measued 1 h later. Intracellular concentrations of injected compounds were estimated by assuming an internal distribution volume of 0.4 µl (Zeuthen et al., 2002).

Measurements of AMG or Uridine Uptake in Oocytes. hSGLT1-mediated AMG uptake was determined by correcting AMG uptake in hSGLT1-expressing oocytes for AMG uptake measured in non-cRNA-injected oocytes which were handled in parallel. Oocytes were incubated for 20 min at room temperature in Ori-buffer containing 25 µM AMG traced with [^{14}C]AMG. Thereafter the oocytes were washed four times with ice-cold Ori-buffer containing 1 mM phlorizin. hCNT1-mediated uridine uptake was determined by measuring the difference of uridine uptake between oocytes in which hCNT1 was expressed by cRNA injection, and non-cRNA-injected oocytes. Oocytes were incubated for 20 min at room temperature with Ori-buffer containing 5 µM uridine traced with [^{3}H]uridine and washed four times with ice-cold Ori buffer. Single oocytes were solubilized in 5% (w/v) SDS and analyzed for radioactivity by scintillation counting.

Measurement of hSGLT1-YFP-mediated Glucose-induced Short-circuit Current in Oocytes. For measurement of glucose-induced short-circuit currents in the two-electrode voltage clamp mode, non-cRNA-injected control oocytes and hSGLT1-YFP expressing oocytes were superfused at room temperature with 10 mM citrate-Tris pH 5.0, containing 30 mM potassium gluconate, 1 mM $LaCl_3$, 1 mM $CaCl_2$ plus 170 mM sorbitol (buffer without glucose), the membrane potential was clamped to -50 mV and the steady-state short-circuit current was measured. Superfusion was switched to buffer with

Molecular Pharmacology Fast Forward. Published on August 23, 2016 as DOI: 10.1124/mol.116.104521
This article has not been copyedited and formatted. The final version may differ from this version.

glucose in which 100 mM of sorbitol was replaced by 100 mM D-glucose, and steady-state short-circuit current at -50 mV was measured again. Glucose-induced currents were determined by subtracting steady-state current in the absence glucose from steady-state current in the presence of 100 mM D-glucose. In non-cRNA injected control oocytes no significant glucose-induced currents were observed.

Quantification of Fluorescence Associated with Oocyte Plasma Membranes. Fluorescence intensity associated with the plasma membrane of hSGLT1-YFP expressing oocytes was measured with a confocal laser scanning microscopy (Leica Microsystems CMS GmbH, Mannheim, Germany) equipped with a Leica HCX IRAPO L25x/095W objective (excitation 514 nm, detection 528-580 nm). The optical plane was set to the equator of the oocyte and the settings of YFP fluorecence acquisition (laser intensity and PMT gain) were kept constant for all tested oocytes. YFP-fluorescence intensity of a quarter circular segment per oocyte was measured using the LAS AF software from Leica.

Incubation of Caco-2 Cells with DFMO and/or hRS1-Reg(S20E) coupled to nanohydrogel. Monolayers of differentiated Caco-2 cells were incubated for 30 min at 37°C with fetal calf serum–free minimal essential medium without addition or with serum-free medium containing 5 mM DFMO, 0.25 mg/ml nanohydrogel, 2.5 ng hRS1-Reg(S20E) linked to 0.25 mg/ml nanohydrogel or DFMO plus hRS1-Reg(S20E) linked to nanohydrogel. Nanohydrogels were synthesized and hRS1-Reg(S20E) was coupled as described (Veyhl-Wichmann et al., 2016) with the exceptions that alloxan was used for oxidation and hydroxyethylacrylate for quenching of free thiol groups (Singh et al, 2013).

Transport Measurements in Caco-2 Cells. Phlorizin-inhibited AMG uptake into Caco-2 cells was measured as described (Kipp et al., 2003). Confluent monolayers of Caco-2 cells were washed three times at 37°C with Hepes buffer (10 mM Hepes pH 7.2, 137 mM NaCl, 4.7 mM KCl, 1.2 mM KH_2PO_4, 1.2 mM $MgSO_4$, 2.5 mM $CaCl_2$) and incubated for 10 min at 37°C with Hepes buffer containing 0.7 µM [^{14}C]AMG or 0.7 µM [^{14}C]AMG plus 1 mM phlorizin. AMG uptake was stopped with ice-cold Hepes buffer containing 1 mM phlorizin and the monolayers were washed with the same buffer. Cells were solubilized with 2% (w/v) SDS and radioactivity was determined by scintillation counting. Difference between AMG uptake in the absence and presence of phlorizin was calculated.

Molecular Pharmacology Fast Forward. Published on August 23, 2016 as DOI: 10.1124/mol.116.104521
This article has not been copyedited and formatted. The final version may differ from this version.

Statistics and Fitting Procedures. In the SPR experiments k_{on} and k_{off} rate constants were obtained by fitting the experimental sensograms of individual experiments employing a simple 1:1 Langmuir-type interaction model. All Chi2 values for the fitted data were less than 10% of the maximal responses. Half maximal concentration values for inhibition of ODC activities (IC_{50}) (Fig. 5A,C) were determined by fitting the Hill equation to the data. K_m values (Fig. 5B) were calculated by fitting the Michaelis Menten equation to the data. The half maximal effective concentration (EC_{50}) for D-glucose-induced protection of ODC activity from inhibition by DFMO (Fig. 5D) was determined by fitting a one-site binding model to the data. Binding constants (k_{on}, k_{off}, K_D), K_m-values, half maximal inhibitory concentrations (IC_{50}), and half maximal effective concentration for glucose activation (EC_{50}) are presented as means ± SD which were obtained by fitting data from individual experiments. In experiments with oocytes (Figs. 6-8) mean values ± SE are indicated. When three or more experimental conditions were compared, significance of differences was determined by ANOVA using posthoc Tukey comparison. Significance of differences of two experimental conditions was determined by Student´s t test. $P < 0.05$ was considered significant.

Results

Ornithine Decarboxylase Binds to an N-terminal Regulatory Domain of hRS1 (*RSC1A1*). We screened a cDNA library from human embryonic kidney for proteins that interact with a polypeptide comprising amino acids 2-312 of hRS1 (hRS1(2-312)) using the two-hybrid split ubiquitin system (Johnsson and Varshavsky, 1994). The identified proteins are indicated in Supplemental Table 1. We characterized the interaction of hRS1(2-312) with hODC1 (Genbank, NP_002530.1) (Kahana and Nathans, 1984) in detail because effects of ODC on SGLT1 activity have been reported (Johnson et al., 1995; Uda et al., 2002).

For coprecipitation of overexpressed proteins, green fluorescent protein (GFP) containing an S-tag fused to the N-terminus of hRS1(2-312) (GFP-S-hRS1(2-312)) was expressed in HEK293 cells together with hODC1 containing a C-terminal myc-tag (hODC1-myc). In cell lysates either GFP-S-hRS1(2-312) was precipitated by S-tag binding to S-protein-agarose and coprecipitation of hODC1-

Molecular Pharmacology Fast Forward. Published on August 23, 2016 as DOI: 10.1124/mol.116.104521
This article has not been copyedited and formatted. The final version may differ from this version.

myc was demonstrated using an antibody against myc (Fig. 1A) or hODC1-myc was precipitated with an anti-myc antibody coupled to agarose and coprecipitation of GFP-S-hRS1(2-312) was demonstrated using an antibody against GFP (Fig. 1B). The specificity of coprecipitation of hODC1 with hRS1(2-312) was confirmed by showing that hODC1-myc did not precipitate together with GFP-S (Fig. 1A) and that GFP-S did not precipitate with hODC1-myc (Fig. 1B).

Recently we observed that hRS1 downregulates the expression of SGLT1 by blocking exocytosis of SGLT1-containing vesicles at the TGN and that this effect is mediated by hRS1-Reg comprising amino acids 16-98 of hRS1 (Veyhl-Wichmann et al., 2016). To determine whether hODC1 binds to hRS1-Reg we expressed either GFP-S-hRS1(2-98) or GFP-S together with hODC1-myc, precipitated ODC1-myc with agarose-coupled anti-myc antibodies, and investigated whether GFP-S or GFP-S-hRS1(2-98) were coprecipitated (Fig. 1C). In contrast to GFP-S, GFP-S-hRS1(2-98) was coprecipitated suggesting that hODC1 binds to hRS1-Reg.

Differentiated CaCo-2 cells which represent an established model for human enterocytes and express SGLT1 (Kipp et al., 2003), were employed to demonstrate association between endogenously expressed, membrane-bound hODC1 and hRS1. To validate hRS1 expression in CaCo-2 cells we performed Western blots with a nuclei- and mitochondria-free cell lysate, a cytosolic fraction, and a total cell membrane fraction using antibody against full-length hRS1 (anti-hRS1-Ab) (Fig. 2A). In the cell lysate and the cytosol protein bands with apparent M_r values of 50k, 31k, 20k and 17k were stained in addition to a 68k M_r-band representing full-length hRS1 (Fig. 2A). Noteworthy anti-hRS1-Ab only stained the 31k M_r-protein in the total cell membrane fraction. When the Western blots were stained with an antibody directed against a peptide within hRS1-Reg (hRS1-Reg-P-Ab), the 68k-, 31k-, 20k-bands were stained in cell the lysate and the cytosol whereas in the total cell membrane fraction only the 31k band was stained (Fig. 2A). The data support our interpretation that RS1-Reg is associated with Golgi membranes (Veyhl-Wichmann et al. 2016). To investigate whether the 31k hRS1-fragment forms a complex with hODC1 we incubated solubilized total cell membranes with a monoclonal antibody against hODC1 and precipitated hODC1 with agarose beads containing a covalently linked antibody against mouse IgG (Fig. 2B). We observed coprecipitation of the 31k M_r-

Molecular Pharmacology Fast Forward. Published on August 23, 2016 as DOI: 10.1124/mol.116.104521
This article has not been copyedited and formatted. The final version may differ from this version.

hRS1 fragment comprising hRS1-Reg with hODC1 indicating *in vivo* association of membrane bound hODC1 with hRS1-Reg.

Demonstration and Characterization of hRS1-Reg Binding to Ornithine Decarboxylase by Surface Plasmon Resonance. To verify and characterize the interaction of hRS1-Reg with hODC1 we performed surface plasmon resonance (SPR) using purified recombinant hODC1 as immobilized ligand and the purified recombinant hRS1-Reg variant proteins hRS1-Reg(S20E) and hRS1-Reg(S20A) as analytes. In these variants phosphorylation at a predicted phosphorylation site is mimicked or prevented by replacement of serine with glutamate or alanine. The peptide hRS1-Reg(S20E) downregulated human SGLT1 (hSGLT1) expressed in *Xenopus laevis* oocytes with a 3,500fold lower half maximal effective concentration (EC_{50}) than hRS1-Reg(S20A) (Veyhl-Wichmann et al., 2016). We also investigated whether the glucose-induced 19,000fold decrease of the EC_{50} of hRS1-Reg(S20E) observed for downregulation of hSGLT1 in oocytes (Veyhl-Wichmann et al., 2016) is reflected by a decreased equilibrium dissociation constant (K_D) value for binding of hRS1-Reg(S20E) to hODC1. Finally we determined whether covalent modification of hODC1 within the substrate binding site by difluoromethylornithine (DFMO), which blocks ODC activity (Grishin et al., 1999), alters binding of hRS1-Reg(S20E).

Human ODC1 (Matsuzawa et al., 2005), the RS1-Reg peptides, and a control peptide comprising amino acids 150-312 of hRS1 were expressed in *E. coli* and purified by affinity chromatography. SDS-PAGE analysis showed that purified hODC1 migrates as a single band with an expected molecular mass of 54 kDa (Pritchard et al., 1982) (Fig. 3A). For the specific enzymatic activity of purified recombinant hODC1 measured at 37°C in the presence of 8 µM ornithine, 0.7 µM of the cosubstrate pyridoxal-5-phosphate and 0.34 mM DTT, a value of 2.9 ± 0.5 µmol CO_2 × mg protein^{-1} × h^{-1} (mean value ± SD, n=3) was obtained. During SDS-PAGE performed in the presence of DTT the purified hRS1-Reg mutants migrate at about 10 kDa representing monomers, whereas the control peptide migrates at about 25 kDa (Fig. 3B). Due to the presence of cysteine residues the hRS1-Reg peptides dimerize in the absence of reducing agents (Fig. 3B), therefore the SPR measurements were performed in the presence of DTT. For SPR analysis purified hODC1 was immobilized on a sensor

Molecular Pharmacology Fast Forward. Published on August 23, 2016 as DOI: 10.1124/mol.116.104521
This article has not been copyedited and formatted. The final version may differ from this version.

chip. The chip was superfused with running buffer (25°C, pH 7.4) containing 150 mM NaCl, 3.5 mM EDTA, 0.005% (v/v) Tween 20, 1 mM DTT and different concentrations of analyzed peptides. For measurements in the presence of glucose or DFMO, either the running buffer was supplemented with 1 mM D-glucose or the immobilized hODC1 was pretreated with 1 mM DFMO.

Both peptides variants, hRS1-Reg(S20A) and hRS1-Reg(S20E), bind with high affinity to hODC1 (Fig. 4, Table 1). For both variants similar association rate constant (k_{on}) values, similar dissociation rate constant (k_{off}) values and similar equilibrium binding dissociation constant (K_D) values were observed. The constants determined for hRS1-Reg(S20E) were not significantly altered by D-glucose and the constants obtained for hRS1-Reg(S20A) were also not significantly changed after modification of hODC1 with the covalently binding inhibitor DFMO (Table 1). The k_{on} values were in the range between 0.5-0.9 $\times 10^4$ $M^{-1}s^{-1}$, the k_{off} values in the range between 0.6-0.9 $\times 10^{-3}$ s^{-1}, and the deduced K_D values in the range between 68-161 nM (Table 1). The K_D value for the hRS1-Reg(S20A)-hODC1 interaction (68 ± 20 nM) was similar to the half maximal effective concentration (EC_{50}) determined for downregulation of hSGLT1 expressed in oocytes (48 ± 8 nM) (Veyhl-Wichmann et al., 2016). In contrast, the K_D value determined for hRS1-Reg(S20E)-hODC1 interaction (102 ± 25 nM) was 5,000 times higher as the EC_{50} value (19 ± 0.2 pM) measured for downregulation of hSGLT1 in oocytes (Veyhl-Wichmann et al., 2016). Furthermore, in contrast to the highly differing EC_{50} values obtained for downregulation of hSGLT1 in the absence and presence of the glucose analogue α-methylglucopyranoside (AMG) (Veyhl-Wichmann et al., 2016), the binding affinities for the peptide-hODC1 interaction were not influenced significantly by glucose.

Demonstration and Characterization of Inhibition of ODC Activity by hRS1-Reg. Next we investigated whether binding of the hRS1-Reg peptides to hODC1 influences the enzymatic activity. We measured the CO_2 generation when 10 ng purified recombinant hODC1 was incubated with hRS1-Reg(S20A) or hRS1-Reg(S20E) in the presence of 8 µM ornithine and 0.7 µM of the cosubstrate pyridoxal-5-phosphate (Fig. 5A). In presence of 10 µM hRS1-Reg(S20A) or hRS1-Reg(S20E) the enzymatic activity was inhibited by 66% or 79%, respectively. For hRS1-Reg(S20A) a half maximal concentration for inhibition (IC_{50}) of 1.10 ± 0.19 µM was calculated whereas for hRS1-Reg(S20E) an

Molecular Pharmacology Fast Forward. Published on August 23, 2016 as DOI: 10.1124/mol.116.104521
This article has not been copyedited and formatted. The final version may differ from this version.

IC_{50} value of 0.27 ± 0.04 µM was determined (mean values ± SD, n = 3 each, $P < 0.001$ for difference). The IC_{50} values obtained for inhibition of hODC1 by hRS1-Reg(S20A) or hRS1-Reg(S20E) are 16fold or 2.6fold higher, compared to the K_D values determined for peptide binding to hODC1 measured by SPR in the absence of substrate and cosubstrate. The lower IC_{50} value of hRS1-Reg(S20E) for inhibition of ODC activity compared to hRS1-Reg(S20A) correlates with the lower EC_{50} value of hRS1-Reg(S20E) versus hRS1-Reg(S20A) observed for downregulation of hSGLT1 in oocytes (Veyhl-Wichmann et al., 2016). This suggests that inhibition of hODC1 by hRS1-Reg is critically involved in hRS1-Reg-mediated downregulation of hSGLT in the plasma membrane.

Previously we observed that the EC_{50} of hRS1-Reg(S20E) for downregulation of SGLT1 in oocytes was 19,000fold decreased in the presence of non-metabolizable glucose analogue AMG (Veyhl-Wichmann et al., 2016). Measuring the inhibition of the enzymatic activity of purified recombinant hODC1 by hRS1-Reg(S20E) in the presence of 1 mM D-glucose (Fig. 5A) we observed a 3fold lower IC_{50} value compared to the absence of glucose (absence of glucose: 0.27 ± 0.04 µM, 1 mM D-glucose: 0.084 ± 0.014 µM, mean value ± SD, n = 3 each, $P < 0.01$). Thus, glucose has a qualitatively similar but quantitatively much smaller effect on IC_{50} for inhibition of hODC1 activity compared to the EC_{50} for downregulation of hSGLT1.

ODC is endogenously expressed in *Xenopus laevis* oocytes (Osborne et al., 1989). In lipid-depleted homogenates prepared from oocytes we measured a specific ODC activity of 83 ± 17 pmol $CO_2 \times$ mg protein$^{-1} \times h^{-1}$ (mean value ± SD, n= 3). To determine whether the observed differences between IC_{50} values obtained with hODC1 and the EC_{50} values for downregulation of SGLT1 in *Xenopus* oocytes are due to different properties of recombinant hODC1 versus endogeneous ODC of *Xenopus laevis*, we measured inhibition of ODC activity by hRS1-Reg(S20E) in the lipid-depleted oocyte homogenates in the absence and presence of 1 mM AMG. The IC_{50} values determined in oocyte homogenates were in the same range of magnitude as the values obtained with purified hODC1 indicating similar efficacy for interaction of hRS1-Reg(S20E) with hODC1 and ODC in oocytes (absence of glucose: 0.66 ± 0.13 µM, 1 mM AMG: 0.23 ± 0.05 µM, mean values ± SD, n = 3 each, *P*

Molecular Pharmacology Fast Forward. Published on August 23, 2016 as DOI: 10.1124/mol.116.104521
This article has not been copyedited and formatted. The final version may differ from this version.

< 0.01). In oocyte homogenates a similar glucose-induced increase of efficacy for inhibition by hRS1-Reg(S20E) was observed as with hODC1.

D-Glucose Decreases Efficacy of DFMO for Inhibition of Enzymatic Reaction. We measured the substrate dependence of the enzymatic activity of purified hODC1 with and without 1 mM D-glucose. Under both conditions Michaelis Menten type kinetics with similar K_m and V_{max} values were obtained (Fig. 5B). In the absence and presence of glucose K_m values of 0.27 ± 0.06 and 0.26 ± 0.06 mM and V_{max} values of 4.0 ± 0.8 and 4.1 ± 0.3 µmol CO_2 × mg protein^{-1} × h^{-1} (mean values ± SD, n=3 each) were determined, respectively. We also measured the inhibition of hODC1 activity by DFMO in the absence or presence of 1 mM D-glucose using 0.1 µg purified recombinant hODC1 × ml^{-1} and a substrate concentration of 8 µM ornithine (Fig. 5C). In the absence of glucose, 0.1 mM DFMO inhibited 95% of the enzymatic activity of hODC1. For inhibition of hODC1 in the presence of 1 mM D-glucose a 2.6 fold higher IC_{50} value was obtained as in the absence of glucose (12.6 ± 2.0 µM versus 32.8 ± 6.8 µM, mean values ± SD, n = 3 each, p < 0.01). For DFMO inhibition of endogenous ODC activity in lipid-depleted oocyte homogenates measured in the absence of glucose using 1 mg protein × ml^{-1} for the enzymatic assay, 1 mM DFMO was required to obtain 90% inhibition. Similar to the glucose effect on DFMO inhibition of purified hODC1 (Fig. 5C) a significantly higher IC_{50} value for inhibition by DFMO was obtained in the presence of 1 mM AMG compared to the absence of glucose (432 ± 79 µM versus 118 ± 13 µM, mean values ± SD, n = 3 each, P < 0.01). The IC_{50} values for DFMO inhibition of ODC in lipid-depleted oocyte homogenates were 9fold higher compared to the IC_{50} values measured with purified hODC1. Because the apparent IC_{50} value for DFMO inhibition determined in lipid-depleted oocyte homogenates was positively correlated with the protein concentration in the assay (data not shown), the higher apparent IC_{50} determined in lipid-depleted oocyte homogenate compared to the IC_{50} of purified hODC1 is probably due to a reduced concentration of free DFMO in oocyte homogenates due to nonspecific binding of DFMO to proteins and/or lipids. We observed that 3 mM DFMO was required to inhibit ODC activity up to 70% in lipid-depleted oocyte homogenates when the assay was performed in the presence of 10 mg protein × ml^{-1}.

Molecular Pharmacology Fast Forward. Published on August 23, 2016 as DOI: 10.1124/mol.116.104521
This article has not been copyedited and formatted. The final version may differ from this version.

Also under this condition ODC inhibition was reduced significantly by addition of 1 mM AMG (data not shown).

To characterize the interaction of glucose with hODC1 we measured the inhibition of purified hODC1 by 12.5 μM DFMO in the presence of different D-glucose concentrations (Fig. 5D). A saturable protective effect of glucose with an EC_{50} of 0.28 ± 0.09 mM (mean value ± SD, n = 3) was observed. The data indicate that ODC contains a glucose binding site.

Effect of ODC Activity on the Expression of hSGLT1-mediated Glucose Transport Expressed in Oocytes. We investigated whether hSGLT1-mediated AMG uptake was increased after coexpression of hODC1 or decreased after inhibition of endogeneous ODC activity by DFMO. After coexpression of hODC1 with hSGLT1 in oocytes the hSGLT1-mediated uptake of 25 μM AMG was increased by 40% (Fig. 6A). We then investigated whether the endogenous ODC activity in oocytes has an effect on hSGLT1-mediated AMG uptake. We expressed hSGLT1 by injection of hSGLT1-cRNA into oocytes and incubation for 2 days, inhibited ODC activity by injection of 3 mM DFMO, and measured AMG uptake one hour later. DFMO inhibited hSGLT1-mediated AMG uptake by 50% (Fig. 6B,C). Importantly the inhibition by DFMO could be counteracted when 1 μM putrescine, the product of ODC-mediated decarboxylation of ornithine, or 1 mM AMG were coinjected with DFMO (Fig. 6C). The data suggest that SGLT1 is upregulated in response to ODC-mediated generation of putrescine and that the upregulation is blunted by glucose binding to ODC.

To elucidate whether ODC influences an exocytotic pathway of hSGLT1 at the TGN like hRS1-Reg (Veyhl-Wichmann et al., 2016), we investigated whether the inhibition of hSGLT1-mediated AMG uptake by DFMO is dependent on Golgi integrity (Fig. 6B). One hour after injection of 12.5 μM brefeldin A (BFA) into hSGLT1-expressing oocytes, hSGLT1-mediated AMG uptake was inhibited by 40 to 50% as described earlier (Veyhl et al., 2006; Veyhl-Wichmann et al., 2016). No further inhibition was observed when 3 mM DFMO was injected together with BFA.

hRS1-Reg Blocks the Exocytotic Pathway of SGLT1 by Inhibiting the Enzymatic Activity of ODC. To determine whether the posttranscriptional short-term regulation of hSGLT1 by ODC and hRS1-Reg is mediated by the same regulatory pathway we investigated whether downregulation of

Molecular Pharmacology Fast Forward. Published on August 23, 2016 as DOI: 10.1124/mol.116.104521
This article has not been copyedited and formatted. The final version may differ from this version.

hSGLT1 by inhibition of ODC and by hRS1-Reg are synergistic. Injection of hRS1-Reg or DFMO into hSGLT1-expressing oocytes inhibited AMG uptake to a similar degree of 40-50%, and the inhibition was not further increased upon coinjection of hRS1-Reg and DFMO (Fig. 7A). To determine whether hRS1-Reg downregulates hSGLT1 via ODC inhibition, we investigated whether hRS1-Reg-mediated downregulation of AMG uptake could be prevented when putrescine was supplemented. Inhibition of hSGLT1-mediated AMG uptake by hRS1-Reg was indeed blunted when 1 μM putrescine was injected (Fig. 7B). The data suggest that downregulation of hSGLT1 by hRS1-Reg is mediated via inhibition of ODC activity. Because hRS1-Reg inhibits the exocytotic pathway of the Na^+-nucleoside cotransporter hCNT1 at the Golgi independently of glucose (Veyhl-Wichmann et al., 2016) we investigated whether ODC activity is also involved in short-term regulation of CNT1. In oocytes expressing hCNT1 sodium-dependent uptake of 5 μM [^{3}H]uridine was not inhibited by DFMO, whereas it was downregulated by hRS1-Reg (Fig. 7C).

DFMO and hRS1-Reg(S20E) Decrease Plasma Membrane Abundance of hSGLT1 Expressed in Oocytes. Based on supporting experimental evidence derived from different experimental approaches we concluded in a recent study that hRS1-Reg downregulates plasma membrane abundance of hSGLT1 (Veyhl-Wichmann et al., 2016). The above described data suggesting that hODC1 is part of the hRS1-Reg-modulated exocytotic pathway, implicate that also DFMO decreases the amount of SGLT1 in the plasma membrane. To demonstrate downregulation of hSGLT1 in the plasma membrane by hRS1-Reg and DFMO directly, we expressed a hSGLT1-YFP fusion protein in oocytes, injected DFMO, hRS1-Reg(S20E) or DFMO plus hRS1-Reg(S20E). After 1 h we measured short-circuit currents at -50 mV that were induced by a saturating D-glucose concentration and determined the concentrations of YFP-hSGLT1 associated with the plasma membrane by measuring YFP fluorescence (Fig. 8). After injection of hRS1-Reg(S20E), DFMO or hRS1-Reg(S20E) plus DFMO, the glucose-induced currents were decreased 40-45% whereas the membrane associated fluorescence measured was decreased 30-36%. The data indicate non-additive downregulation of SGLT1 abundance in the plasma membrane by hRS1-Reg(S20E) and DFMO. The slightly smaller

Molecular Pharmacology Fast Forward. Published on August 23, 2016 as DOI: 10.1124/mol.116.104521
This article has not been copyedited and formatted. The final version may differ from this version.

effects on fluorescence compared to glucose-induced currents may be due to some plasma membrane-associated transporter that is not functional.

DFMO and hRS1-Reg(S20E) Decrease Phlorizin-inhibited AMG Uptake in Caco-2 Cells. To evaluate the physiological relevance of RS1/ODC regulated membrane trafficking of SGLT1 in small intestine we investigated the effects of DFMO and hRS1-Reg(S20E) on transport function of hSGLT1 in differentiated Caco-2 cells. Differentiated Caco-2 cells grown in the presence of 1 mM D-glucose, were incubated for 30 min at 37^{o}C with 0.25 mg/ml nanohydrogel, 0.25 ng/ml of hRS1-Reg(S20E) linked to 0.25 mg/ml nanohydrogel, 5 mM DFMO or hRS1-Reg(S20E) linked to nanohydrogel plus DFMO. The employed concentration of nanohydrogel coupled with hRS1-Reg(S20E) was optimized to induce a maximal decrease of phlorizin-inhibited AMG uptake after 30 min incubation. After washing of the incubated cells, phlorizin-inhibited uptake of 5 μM [^{14}C]AMG was measured (Fig. 9). DFMO, hRS1-Reg(S20E) and DFMO plus hRS1-Reg(S20E) decreased phlorizin-inhibited AMG uptake by similar degrees. The downregulation of transport by DFMO and hRS1-Reg(20E) were not additive. The data suggest in vivo relevance of RS1/ODC-mediated short-term regulation of SGLT1 in small intestine.

Discussion

Previously we reported that differentially phosphorylated forms of RS1-Reg induce blockage of the release of vesicles that contain either SGLT1 or CNT1 from the TGN, and that this regulation alters transporter activity in the plasma membrane within minutes (Veyhl-Wichmann et al., 2016). We showed that short-term downregulation of SGLT1 by RS1-Reg is glucose dependent. On the basis of these data the hypothesis was raised that differently phosphorylated forms of RS1-Reg bind to different receptor proteins at the TGN, which steer release of different vesicle populations.

In the present work we provide evidence that hODC1 is the receptor protein for hRS1-Reg that controls the exocytotic pathway of SGLT1. We showed that an N-terminal hRS1-fragment containing hRS1-Reg that is associated with membranes, interacts with membrane-bound hODC1. SPR analysis of purified recombinant hODC1 with hRS1-Reg variants in which phosphorylation of a motif that is

Molecular Pharmacology Fast Forward. Published on August 23, 2016 as DOI: 10.1124/mol.116.104521
This article has not been copyedited and formatted. The final version may differ from this version.

critical for the efficacy of SGLT1 versus CNT1 regulation was prevented (hRS1-Reg(S20A)) or mimicked (hRS1-Reg(S20E)), revealed high affinity binding to hODC1 with similar K_D values of about 100 nM. Whereas the K_D for binding of hRS1-Reg(S20A) to hODC1 was similar to the EC_{50} determined for downregulation of expressed hSGLT1 in oocytes, the K_D for binding of hRS1-Reg(S20E) to hODC1 was three orders of magnitude lower compared to EC_{50} required for downregulation of hSGLT1 in oocytes.

Our observation that enzymatic activity of hODC1 was inhibited by hRS1-Reg variants and that the IC_{50} for inhibition by hRS1-Reg(S20E) was similar to the K_D for binding, suggests that binding of RS1-Reg to ODC is mechanistically linked to inhibition of enzymatic activity. The 16fold higher IC_{50} for inhibition of hODC1 by hRS1-Reg(S20A) compared to the K_D for binding of hRS1-Reg(S20A) suggests an influence of the experimental conditions such as absence of substrate and cosubstrate in the SPR measurements. Importantly, we observed qualitatively similar effects on IC_{50} values for inhibition of hODC1 and EC_{50} values for regulation of hSGLT1 in oocytes in response to mutation of hRS1-Reg at position 20, and in response to addition of glucose during treatment with hRS1-Reg(S20E). In addition we demonstrated that hODC1 contains a glucose binding site. The qualitatively similar effects of a mutation in hRS1-Reg and of glucose on enzymativ activity of hODC1 and downregulation of hSGLT1 suggest a central role of ODC1 in the RS1-Reg-induced, glucose-dependent short-term regulation of SGLT1.

The reason for the orders of magnitude lower EC_{50} value of hRS1-Reg(S20E)-induced down-regulation of hSGLT1 in oocytes compared to the IC_{50} for inhibition of purified hODC1 is not understood. Because we observed a similar IC_{50} value in oocyte homogenates as with hODC1, species difference of ODC can be excluded. We speculate that ODC1 at the TGN has a different conformation than ODC1 in the cytosol. This may be due to association of ODC1 with the TGN membrane and/or a TGN protein.

Employing *Xenopus laevis* oocytes in which hSGLT1 was expressed, we provided evidence that the inhibition of ODC activity by hRS1-Reg mediates downregulation of the exocytotic pathway of SGLT1. Blocking of this pathway for 1 h leads to an 40-50% reduction of hSGLT1 abundance in the

Molecular Pharmacology Fast Forward. Published on August 23, 2016 as DOI: 10.1124/mol.116.104521
This article has not been copyedited and formatted. The final version may differ from this version.

plasma membrane. The oocytes do not express endogenous RS1 (Vernaleken et al., 2007; Veyhl-Wichmann et al., 2016) but express endogenous ODC (Osborne et al., 1989). We observed that inhibition of ODC activity in oocytes by DFMO downregulated hSGLT1 in the plasma membrane within one hour to a similar degree as after dissociation of the Golgi with BFA, that the effects of DFMO and BFA are not additive, and that downregulation of hSGLT1 by DFMO was not observed when putrescine, the product of the enzymatic reaction of ODC, was added. We also showed that downregulation of hSGLT1 expressed in oocytes by hRS1-Reg and DFMO was not additive, and that downregulation of hSGLT1 by RS1-Reg was prevented by putrescine.

Since cloning of mammalian ODC (Kahana and Nathans, 1984) properties, functions and biomedical impact of ODC have been studied extensively. ODC is the rate-limiting enzyme of polyamine biosynthesis and is critically involved in polyamine-dependent regulation of cell growth, transformation and differentiation (Wallace et al., 2003). The intracellular concentration and enzymatic activity of ODC is regulated on transcriptional, translational and posttranslational levels (Pegg, 2006). ODC is a pyridoxal-5-phosphate-dependent amino acid decarboxylase which is functionally active as homodimer. Regulations of proteosomal degradation of ODC and of the equilibrium between functionally active dimers and inactive monomers have been described. Proteins called antizymes (AZ1, AZ2 and AZ3) and antizyme inhibitors (AZIN1 and AZN2) are involved (Mangold and Leberer, 2005; Pegg, 2006). Antizyme binds to ODC monomers and thereby decreases the number of functionally active ODC dimers. Antizyme-ODC monomer complexes are directed to the 26S proteasome where ODC is degraded independent of ubiquitinylation, whereas antizyme is recycled (Coleman et al., 1994; Hayashi and Murakami, 1995; Mangold, 2005). Antizyme inhibitor is highly homologous to ODC but has no enzymatic activity (Murakami et al., 1996; Mangold and Leberer, 2005). It binds tightly to antizyme and thereby prevents its association with ODC monomers. This leads to an increase of functionally active ODC dimers.

Previous data have suggested mutual interrelations between ODC and SGLT1. For instance, it has been described that polyamines influence the expression and membrane abundance of SGLT1 during cell differentiation of LLC-PK_1 cells (Peng and Lever, 1993; Wild et al., 2007). On the other hand it

Molecular Pharmacology Fast Forward. Published on August 23, 2016 as DOI: 10.1124/mol.116.104521
This article has not been copyedited and formatted. The final version may differ from this version.

has been reported that AMG stimulates ODC mRNA expression in LLC-PK_1 cells (Benis and Lundgren, 1993). In the small intestine posttranslational regulation of SGLT1 by ODC and/or polyamines has been described. One study reported that glucose uptake into brush-border membrane vesicles isolated from rabbit small intestine was increased independently from protein synthesis when the animals had received polyamines with drinking water 24 h earlier, whereas glucose uptake was decreased upon application of DFMO (Johnson et al., 1995). Rapid posttranslational upregulation of SGLT1 in the brush-border membrane was observed 15 min after luminal application of polyamines (Uda et al., 2002). This effect might be due to RS1/ODC-mediated regulation of SGLT1 at the TGN described in the present report.

On the basis of our data we propose a mechanism for this regulation as depicted in Fig. 10: A population of ODC is located or activated at or close to TGN regions where budding of SGLT1-containing vesicles occurs. Dynamin and caveolin may be involved in budding, because RS1-dependent regulation of the exocytotic pathway of SGLT1 is dynamin-dependent (Veyhl et al., 2003), and SGLT1 colocalizes with dynamin at the TGN (Kroiss et al., 2006). In addition a caveolin-dependent exocytotic pathway of SGLT1, which can be inhibited by BFA, has been described (Elvira et al., 2013). After activation of ODC the local concentration of putrescine is increased. On the basis of our data we hypothesize that the release of SGLT1-containing vesicles from the Golgi is activated by putrescine and/or other polyamines (Fig. 10). Because in non-dividing cells the intracellular concentration of free polyamines is very low (Shin et al., 2006), the local generation of putrescine by ODC allows a local activation of polyamine-dependent processes. Due to the wide spread intracellular distribution of ODC protein it is difficult to distinguish specific subcellular ODC locations. This may be the reason why the location of ODC at the TGN has not yet been identified (Schipper et al., 2004). However, it has been shown that antizyme inhibitor 2 (AZIN2) is located at TGN, and data have been presented suggesting that AZIN2 acts as regulator of vesicle trafficking via activation of ODC (Parkkinen et al., 1997; Kanerva et al., 2010). In human a high mRNA expression of AZIN2 mRNA has been observed in brain and testis, whereas only minor expression was detected in kidney and the gastrointestinal tract (Pitkänen et al., 2001). Performing RT-PCR with mouse tissues we showed that

Molecular Pharmacology Fast Forward. Published on August 23, 2016 as DOI: 10.1124/mol.116.104521
This article has not been copyedited and formatted. The final version may differ from this version.

AZIN2 is also expressed in duodenum and jejunum (C. Chintalapati and H. Koepsell, unpublished data). After selective activation of RS1-Reg by protein kinases, binding of RS1 to ODC blocks its enzymatic activity, which leads to decreased release of SGLT1-containing vesicles from the TGN (Fig. 10). At high intracellular concentrations of D-glucose, glucose binds to ODC. This possibly leads to a conformational change, which decreases the affinity of RS1 to ODC and blunts the inhibitory effect of RS1-Reg binding on ODC activity.

Our data show that ODC mediates release from the TGN, however, it remains a challenge to determine the specific functional properties of ODC at the TGN and to elucidate how a local increase of polyamines at the TGN induces vesicle release. The identification of a new functional role of ODC, and a high-affinity binding site for hRS1-Reg in ODC where inhibition of enzymatic activity can be induced, has provided a new pharmacological target for medical interventions. For example, RS1-Reg-derived ODC inhibitors that downregulate SGLT1-mediated glucose uptake in small intestine may be useful for the treatment of diabetes (Powell et al., 2013; Song et al. 2016).

Acknowledgements

We thank M. Lohse (Institute of Pharmacology and Toxicology, University Würzburg) for providing laboratory space and giving technical support. We also thank Dr. Guiliano Ciarimboli (Medizinische Klinik und Poliklinik D, Universitätsklinkum Münster, Münster, Germany) for providing us with tools for split ubiquitin interaction analysis and Dr. S. Matsuzawa (Burnham Institute for Medical Research, La Jolla, USA) for providing us with a vector containing ODC.

Authors Contributions

Participated in research design: Chintalapati, Keller, Mueller, Geiger, Groll, Gorboulev, Koepsell.

Conducted experiments: Chintalapati, Keller, Mueller, Schäfer, Veyhl-Wichmann.

Contributed to new reagents or analytic tools: Chintalapati, Keller, Gorboulev, Groll, Zilkowski, Geiger.

Performed data analysis: Chintalapati, Keller, Mueller, Schäfer, Veyhl-Wichmann, Koepsell.

Wrote or contributed to the writing of the manuscript: Koepsell.

Molecular Pharmacology Fast Forward. Published on August 23, 2016 as DOI: 10.1124/mol.116.104521
This article has not been copyedited and formatted. The final version may differ from this version.

References

Benis RC and Lundgren DW (1993) Sodium-dependent co-transported analogues of glucose stimulate ornithine decarboxylase mRNA expression in LLC-PK_1 cells. *Biochem J* **289**:751-756.

Brast S, Grabner A, Sucic S, Sitte HH, Hermann E, Pavenstadt H, Schlatter E, and Ciarimboli G (2012) The cysteines of the extracellular loop are crucial for trafficking of human organic cation transporter 2 to the plasma membrane and are involved in oligomerization. *FASEB J* **26**:976-986.

Busch AE, Quester S, Ulzheimer J C, Waldegger S, Gorboulev V, Arndt P, Lang F, and Koepsell H (1996) Electrogenic properties and substrate specificity of the polyspecific rat cation transporter rOCT1. *J Biol Chem* **271**:32599-32604.

Coleman CS, Stanley BA, Viswanath R, and Pegg AE (1994) Rapid exchange of subunits of mammalian ornithine decarboxylase. *J Biol Chem* **269**:3155-3158.

Elvira B, Honisch S, Almilaji A, Pakladok T, Liu G, Shumilina E, Alesutan I, Yang W, Munoz C, and Lang F (2013) Up-regulation of Na^+-coupled glucose transporter SGLT1 by caveolin-1. *Biochim Biophys Acta* **1823**:2394-2398.

Errasti-Murugarren E, Fernandez-Calotti P, Veyhl-Wichmann M, Diepold M, Pinilla-Macua I, Perez-Torras S, Kipp H, Koepsell H, and Pastor-Anglada M (2012) Role of the transporter regulator protein (RS1) in the modulation of concentrative nucleoside transporters (CNTs) in epithelia. *Mol Pharmacol* **82**:59-67.

Filatova A, Leyerer M, Gorboulev V, Chintalapati C, Reinders Y, Müller T D, Srinivasan A, Hübner S, and Koepsell H (2009) Novel shuttling domain in a regulator (*RSC1A1*) of transporter SGLT1 steers cell cycle-dependent nuclear location. *Traffic* **10**:1599-1618.

Gorboulev V, Schürmann A, Vallon V, Kipp H, Jaschke A, Klessen D, Friedrich A, Scherneck S, Rieg T, Cunard R, Veyhl-Wichmann M, Srinivasan A, Balen D, Breljak D, Rexhepaj R, Parker HE, Gribble FM, Reimann F, Lang F, Wiese S, Sabolic I, Sendtner M, and Koepsell H (2012) Na^+-D-glucose cotransporter SGLT1 is pivotal for intestinal glucose absorption and glucose-dependent incretin secretion. *Diabetes* **61**:187-196.

Grant SG, Jessee J, Bloom FR, and Hanahan D (1990) Differential plasmid rescue from transgenic mouse DNAs into *Escherichia coli* methylation-restriction mutants. *Proc Natl Acad Sci U S A* **87**:4645-4649.

Grishin NV, Osterman AL, Brooks HB, Phillips MA, and Goldsmith EJ (1999) X-ray structure of ornithine decarboxylase from *Trypanosoma brucei*: the native structure and the structure in complex with alpha-difluoromethylornithine. *Biochemistry* **38**:15174-15184.

Hayashi S and Murakami Y (1995) Rapid and regulated degradation of ornithine decarboxylase. *Biochem J* **306**:1-10.

Johnson LR, Brockway PD, Madsen K, Hardin JA, and Gall DG (1995) Polyamines alter intestinal glucose transport. *Am J Physiol* **268**:G416-G423.

Johnsson N and Varshavsky A (1994) Split ubiquitin as a sensor of protein interactions in vivo. *Proc Natl Acad Sci U S A* **91**:10340-10344.

Kahana C and Nathans D (1984) Isolation of cloned CDNA encoding mammalian ornithine decarboxylase. *Proc Natl Acad Sci U S A* **81**:3645-3649.

Kanerva K, Makitie LT, Back N, and Andersson LC (2010) Ornithine decarboxylase antizyme inhibitor 2 regulates intracellular vesicle trafficking. *Exp Cell Res* **316**:1896-1906.

Keller T, Elfeber M, Gorboulev V, Reiländer H, and Koepsell H (2005) Purification and functional reconstitution of the rat organic cation transporter OCT1. *Biochemistry* **44**:12253-12263.

Kipp H, Khoursandi S, Scharlau D, and Kinne RKH (2003) More than apical: distribution of SGLT1 in Caco-2 cells. *Am J Physiol Cell Physiol* **285**: C737-C749.

Korn T, Kühlkamp T, Track C, Schatz I, Baumgarten K, Gorboulev V, and Koepsell H (2001) The plasma membrane-associated protein RS1 decreases transcription of the transporter SGLT1 in confluent LLC-PK_1 cells. *J Biol Chem* **276**: 45330-45340.

Kroiss M, Leyerer M, Gorboulev V, Kühlkamp T, Kipp H, and Koepsell H (2006) Transporter regulator RS1 *(RSC1A1)* coats the *trans*-Golgi network and migrates into the nucleus. *Am J Physiol Renal Physiol* **291**:F1201-F1212.

Molecular Pharmacology Fast Forward. Published on August 23, 2016 as DOI: 10.1124/mol.116.104521
This article has not been copyedited and formatted. The final version may differ from this version.

Lambotte S, Veyhl M, Köhler M, Morrison-Shetlar AI, Kinne RKH, Schmid M, and Koepsell H (1996) The human gene of a protein that modifies Na^+-D-glucose co-transport. *DNA Cell Biol* **15**:769-777.

Mangold U (2005) The antizyme family: polyamines and beyond. *IUBMB Life* **57**:671-676.

Mangold U and Leberer E (2005) Regulation of all members of the antizyme family by antizyme inhibitor. *Biochem J* **385**:21-28.

Matsuzawa S, Cuddy M, Fukushima T, and Reed JC (2005) Method for targeting protein destruction by using a ubiquitin-independent, proteasome-mediated degradation pathway. *Proc Natl Acad Sci U S A* **102**:14982-14987.

Milovic V, Turhanowa L, Fares FA, Lerner A, Caspary WF and Stein J (1998) S-adenosylmethionine decarboxylase activity and utilization of exogenous putrescine are enhanced in colon cancer Cells stimulated to grow by EGF. *Z Gastroenterol* **36**:947-954.

Murakami Y, Ichiba T, Matsufuji S, and Hayashi S (1996) Cloning of antizyme inhibitor, a highly homologous protein to ornithine decarboxylase. *J Biol Chem* **271**:3340-3342.

Nour-Eldin HH, Hansen BG, Norholm MH, Jensen JK, and Halkier BA (2006). Advancing uracil-excision based cloning towards an ideal technique for cloning PCR fragments. *Nucleic Acids Res* **34**: e122.

Obrdlik P, El-Bakkoury M, Hamacher T, Cappellaro C, Vilarino C, Fleischer C, Ellerbrok H, Kamuzinzi R, Ledent V, Blaudez D, Sanders D, Revuelta JL, Boles E, Andre B, and Frommer WB (2004) K^+ channel interactions detected by a genetic system optimized for systematic studies of membrane protein interactions. *Proc Natl Acad Sci U S A* **101**:12242-12247.

Osborne HB, Mulner-Lorillon O, Marot J, and Belle R (1989) Polyamine levels during Xenopus laevis oogenesis: a role in oocyte competence to meiotic resumption. *Biochem Biophys Res Commun* **158**:520-526.

Osswald C, Baumgarten K, Stümpel F, Gorboulev V, Akimjanova M, Knobeloch K-P, Horak I, Kluge R, Joost H-G, and Koepsell H (2005) Mice without the regulator gene *Rsc1A1* exhibit increased Na^+-D-glucose cotransport in small intestine and develop obesity. *Mol Cell Biol* **25**:78-87.

Parkkinen JJ, Lammi M J, Agren U, Tammi M, Keinänen TA, Hyvönen T, and Eloranta TO (1997) Polyamine-dependent alterations in the structure of microfilaments, Golgi apparatus, endoplasmic reticulum, and proteoglycan synthesis in BHK cells. *J Cell Biochem* **66**:165-174.

Pegg AE (2006) Regulation of ornithine decarboxylase. *J Biol Chem* **281**:14529-14532.

Peng H and Lever JE (1993) Polyamine regulation of Na^+/glucose symporter expression in LLC-PK1 cells. *J Cell Physiol* **154**:238-247.

Pitkänen LT, Heiskala M, and Andersson LC (2001) Expression of a novel human ornithine decarboxylase-like protein in the central nervous system and testes. *Biochem Biophys Res Commun* **287**:1051-1057.

Powell DR, Smith M, Greer J, Harris A, Zhao S, DaCosta C, Mseeh F, Shadoan MK, Sands A, Zambrowicz B, and Ding ZM (2013) LX4211 increases serum glucagon-like peptide 1 and peptide YY levels by reducing sodium/glucose cotransporter 1 (SGLT1)-mediated absorption of intestinal glucose. *J Pharmacol Exp Ther* **345**:250-259.

Pritchard ML, Pegg AE, and Jefferson LS (1982) Ornithine decarboxylase from hepatoma cells and a variant cell line in which the enzyme is more stable. *J Biol Chem* **257**:5892-5899.

Reinhardt J, Veyhl M, Wagner K, Gambaryan S, Dekel C, Akhoundova A, Korn T, and Koepsell H (1999) Cloning and characterization of the transport modifier RS1 from rabbit which was previously assumed to be specific for Na^+-D-glucose cotransport. *Biochim Biophys Acta* 1417:131-143.

Schipper RG, Cuijpers VMJI, De Groot LHJM, Thio M, and Verhofstad AAJ (2004) Intracellular localization of ornithine decarboxylase and its regulatory protein, antizyme-1. *J Histochem Cytochem* **52**:1259-1266.

Shin M, Hirokawa K, and Fujiwara K (2006) Immunoelectron microscopic study of polyamines in the gastrointestinal tract of rat. *Histochem Cell Biol* **125**:369-375.

Singh S., Zilkowski I, Ewald A, Maurell-Lopez T, Albrecht K, Möller M, and Groll J (2013) Mild oxidation of thiofunctional polymers to cytocompatible and stimuli-sensitive hydrogels and nanogels. *Macromol.Biosci.***13**:470-482.

Song P, Onishi A, Koepsell H, and Vallon V (2016) Sodium glucose transporter SGLT1 as therapeutic target in diabetes mellitus. *Expert Opin Ther Targets* doi.org/10.1517/14728222

Uda K, Tsujikawa T, Ihara T, Fujiyama Y, and Bamba T (2002) Luminal polyamines upregulate transmural glucose transport in the rat small intestine. *J Gastroenterol* **37**:434-441.

Vernaleken A, Veyhl M, Gorboulev V, Kottra G, Palm D, Burckhardt B-C, Burckhardt G, Pipkorn R, Beier N, van Amsterdam C, and Koepsell H (2007) Tripeptides of RS1 *(RSC1A1)* inhibit a monosaccharide-dependent exocytotic pathway of Na^+-D-glucose cotransporter SGLT1 with high affinity. *J Biol Chem* **282**:28501-28513.

Veyhl M, Spangenberg J, Püschel B, Poppe R, Dekel C, Fritzsch G, Haase W, and Koepsell H (1993) Cloning of a membrane-associated protein which modifies activity and properties of the Na^+-D-glucose cotransporter. *J Biol Chem* **268**:25041-25053.

Veyhl M, Wagner C A, Gorboulev V, Schmitt B M, Lang F, and Koepsell H (2003) Downregulation of the Na^+-D-glucose cotransporter SGLT1 by protein RS1 (*RSC1A1*) is dependent on dynamin and protein kinase C. *J Membr Biol* **196**:71-81.

Veyhl M, Keller T, Gorboulev V, Vernaleken A, and Koepsell H (2006) RS1*(RSC1A1*) regulates the exocytotic pathway of Na^+-D-glucose cotransporter SGLT1. *Am J Physiol Renal Physiol* **291**:F1213-F1223.

Veyhl-Wichmann M, Friedrich A, Vernaleken A, Singh S, Kipp H, Gorboulev V, Keller T, Chintalapati C, Pipkorn R, Pastor-Anglada M, Groll J, and Koepsell H (2016) Phosphorylation of RS1 (*RSC1A1*) steers inhibition of different exocytotic pathways for glucose transporter SGLT1 and nucleoside transporter CNT1 and an RS1-derived peptide inhibits glucose absorption. *Mol Pharmacol* **89**:118-132.

Wallace HM, Fraser AV, and Hughes A (2003) A perspective of polyamine metabolism. *Biochem J* **376**:1-14.

Wild GE, Searles L E, Koski K G, Drozdowski L A, Begum-Hasan J, and Thomson ABR (2007) Oral polyamine administration modifies the ontogeny of hexose transporter gene expression in the postnatal rat intestine. *Am J Physiol Gastrointest Liver Physiol* **293**:G453-G460.

Wright EM, Hirsch J R, Loo DDF, and Zampighi GA (1997) Regulation of Na^+-/glucose cotransporters. *J Exp Biol* **200**:287-293.

Zeuthen T, Zeuthen E, and Klaerke DA (2002) Mobility of ions, sugar, and water in the cytoplasm of *Xenopus* oocytes expressing Na^+-coupled sugar transporters (SGLT1). *J Physiol* **542**:71-87.

Molecular Pharmacology Fast Forward. Published on August 23, 2016 as DOI: 10.1124/mol.116.104521
This article has not been copyedited and formatted. The final version may differ from this version.

Footnotes

The study was funded by the Deutsche Forschungsgemeinschaft [grant SFB 487/C1].

C.C. and T.K. contributed equally to the work.

Address correspondence to: Hermann Koepsell, Department of Molecular Plant Physiology and Biophysics, Julius-von-Sachs-Institute, Julius-von-Sachs-Platz 2, 97082 Würzburg, Germany, E-mail: Hermann@koepsell.de

This article has supplemental material available at molpharm.aspetjournals.com.

Molecular Pharmacology Fast Forward. Published on August 23, 2016 as DOI: 10.1124/mol.116.104521
This article has not been copyedited and formatted. The final version may differ from this version.

Legends to Figures

Fig. 1. Coprecipitation of N-terminal fragments of hRS1 with human ODC1 in HEK 293 cells with overexpressed proteins. GFP-S, GFP-S-hRS1(2-312) and GFP-S-hRS1(2-98) were expressed in HEK 293 cells together with hODC1-myc. Cells were lysed, cell debris was removed and either GFP-S was precipitated by S-protein agarose (S-protein-AG) or hODC1-myc was precipitated by anti-myc antibodies coupled to agarose (anti-myc-Ab-Ag). The precipitated agarose beads were washed and bound proteins were released by SDS and analysed in Western blots using an antibody against myc (anti-myc-Ab) or an antibody against GFP (anti-GFP-Ab). (A) Coprecipitation of hODC1-myc with GFP-S-hRS1(2-312) using GFP-S as control. hODC1-myc in the SDS-eluted proteins is stained. (B) Coprecipitation of GFP-S-hRS1(2-312) with hODC1-myc using GFP-S as control. GFP-hRS1(2-312) in the SDS-eluted proteins is stained. (C) Coprecipitation of GFP-S-hRS1(2-98) with hODC1-myc using GFP-S as control. GFP-S-hRS1(2-98) in SDS-eluted proteins is stained.

Fig. 2. Analysis of hRS1 and hRS1-fragments in subcellular fractions of Caco-2 cells (A) and coprecipitation of hODC1 and hRS1-Reg (B). (A) Differentiated Caco-2 cells were dissociated and nuclei and organelles were removed by centrifugation (cleared lysate). Cytosol and total cell membranes were separated by centrifuging of the cleared lysate at 100,000 × g. The cellular fractions were characterized by SDS-PAGE and Western blotting. The blots were stained with antibodies against full-length hRS1 (anti-hRS1-Ab) or against a peptide within hRS1-Reg (anti hRS1-Reg-P-Ab) using purified full-length hRS1 (S-hRS1-H) as control. (B) For analysis of proteins that are associated with hODC1, solubilized total membranes (sol. total cell membranes) or solubilization buffer were incubated with anti hODC1-Ab and agarose beads containing covalently linked mouse IgG, and the beads were pelleted. Non-covalently bound proteins were removed from the beads incubated with solubilized total cell membranes (Ag-eluate) or solubilzation buffer (Ag-eluate control). The Western blots were stained with anti-hODC1-Ab raised in mouse and anti-hRS1-Reg-P-Ab raised in rabbit and secondary antibodies against mouse IgG and rabbit IgG, respectively. The high molecular mass bands in the eluates stained with anti-hODC1-Ab represent eluted hODC1-Ab which is stained with the anti-

Molecular Pharmacology Fast Forward. Published on August 23, 2016 as DOI: 10.1124/mol.116.104521
This article has not been copyedited and formatted. The final version may differ from this version.

mouse IgG antibody. 10 µg (cleared lysate, cytosol, total cell membranes, sol. total cell membranes) or 2 µg (eluates, purified proteins) were applied per lane.

Fig. 3. SDS-PAGE of purified recombinant hODC1, hRS1-Reg mutants and control peptide hRS1(150-312). (A) Purification of recombinant hODC1 expessed in *E. coli* as thrombin-cleavable GST-hODC1 fusion protein. After protein expression bacteria were lysed and centrifuged for 1 h at 100,000 × g. The supernatant (cleared lysate) was incubated for 1 h with glutathione-sepharose 4B, the suspension was centrifuged for 5 min at 500 × g and the supernatant (GST lysate) was removed. The resin was washed and incubated for 2 h at 37°C with thrombin to release hODC1. After centrifugation at 500 × g purified hODC1 was retrieved from the supernatant. The samples were subjected to SDS-PAGE analysis. The gel was stained with Coomassie Brilliant Blue. Per lane 10 µg (lysates) or 2 µg of protein (purified hOCD1) were applied. (B) SDS-PAGE of purified recombinant hRS1-Reg(S20A) and hRS1-Reg(S20E) containing an N-terminal cysteine, and of hRS1(150-312) containing a C-terminal His-tag. After affinity purification the samples were dialysed against buffer containing 1 mM DTT (+DTT) or against buffer without DTT (øDTT). For SDS-PAGE the purified proteins were incubated with buffer containing 100 mM DTT (+DTT) or with buffer without DTT (øDTT). 2 µg of polypeptide were applied per lane. The SDS-PAGE gel was stained with Coomassie Brilliant Blue. Data from two different gels are shown.

Fig. 4. SPR analysis of hRS1-Reg(S20A) binding to hODC1. Purified hODC1 was immobilized on a biosensorchip and perfused with different concentrations of hRS1-Reg(S20A) (A) or control peptide hRS1(150-312) (B). The injection of the peptides was started at time point 0 and lasted for 120 s, thereafter perfusion was switched to running buffer to record data of the dissociation phase. The concentrations of the peptides are indicated in nM. (A) Raw data are shown in black, fitted curves are indicated in red.

Fig. 5. Effects of hRS1-Reg mutants and DFMO in absence and presence of glucose on hODC1 activity. CO_2 liberation after addition of ornithine by purified recombinant hODC1 was measured at 37°C in presence of 0.7 µM pyridoxal-5-phosphate, 0.34 mM DTT, hRS1-Reg(S20A), hRS1-Reg(S20E), DFMO and/or D-glucose. (A) Effects of hRS1-Reg(S20A) and hRS1-Reg(S20E) in the absence of glucose and of hRS1-Reg(S20E) in the presence of 1 mM D-glucose on the enzymatic

Molecular Pharmacology Fast Forward. Published on August 23, 2016 as DOI: 10.1124/mol.116.104521
This article has not been copyedited and formatted. The final version may differ from this version.

activity of hODC1 at 8 μM ornithine. (B) Substrate dependence of hODC1-mediated ODC activity in the absence and presence of 1 mM D-glucose. (C) Concentration dependence of the inhibition of hODC1-mediated CO_2 liberation in the presence of 8 μM ornithine by DFM0 in the absence and presence of 1 mM D-glucose. (D) Glucose dependence for glucose protection of inhibition of hODC1 by DFMO. Inhibition of hODC1-mediated CO_2 liberation in the presence of 8 μM ornithine by 12.5 μM DFMO was measured in the presence of different concentrations of D-glucose, and the protective effect of D-glucose on the inhibition was calculated. Mean values ± SE of 9 measurements from 3 independent experiments are shown. The indicated curves were obtained by fitting the Hill equation (A,C), the Michaelis Menten equation (B) or a one-site binding model (D) to the compiled data sets.

Fig. 6. ODC activity regulates hSGLT1-mediated AMG uptake expressed in oocytes via an exocytotic pathway. hSGLT1 or hSGLT1 and hODC1 were expressed in oocytes by injection of cRNAs and incubation for 2 days. hSGLT1-mediated uptake of 25 μM [^{14}C]AMG was measured directly or one hour after injection of 1.2 nmol DFMO, 5 pmol BFA, 0.4 pmol putrescine and/or 1.25 nmol AMG. **(**A) hSGLT1-mediated AMG uptake is upregulated by coexpression of hODC1. hSGLT1 or hSGLT1 plus hODC1 were expressed in oocytes by cRNA injections and 2 days incubation and AMG uptake was measured. (B) Downregulation of hSGLT1 by inhibition of ODC with DFMO is dependent on the Golgi integrity. DFMO, BFA or DFMO plus BFA was(were) injected into hSGLT1-expressing oocytes and AMG uptake was measured 1 h later. (C) hSGLT1-mediated AMG uptake is downregulated by inhibition of endogeneously expressed ODC with DFMO and the DFMO effect is blunted by 1 μM putrescine or 1 mM AMG. DFMO, putrescine or DFMO plus putrescine was (were) injected into hSGLT1-expressing oocytes and AMG uptake was measured after 1 h. Mean values ± SE of 25-30 oocytes from three independent experiments are shown. $^{\bullet\bullet\bullet}P < 0.001$ Students t-test; $^{*}P < 0.05$, $^{**}P < 0.01$ $^{***}P < 0.001$ ANOVA with post hoc Tukey comparison.

Fig. 7. ODC and hRS1-Reg regulate hSGLT1-mediated AMG uptake expressed in oocytes via the same exocytotic pathway. hSGLT1 or hCNT1 were expressed in oocytes by injection of cRNAs and

Molecular Pharmacology Fast Forward. Published on August 23, 2016 as DOI: 10.1124/mol.116.104521
This article has not been copyedited and formatted. The final version may differ from this version.

incubation for 2 days. Either hSGLT1-mediated uptake of 2 5 μM [^{14}C]AMG or hCNT1-mediated uptake of 5 μM [^{3}H]uridine was measured directly or one hour after injection of 1.4 pmol hRS1-Reg, 1.2 nmol DFMO and/or 0.4 pmol putrescine. (A) Downregulation of hSGLT1 by hRS1-Reg and by DFMO are not additive. hRS1-Reg, DFMO or hRS1-Reg plus DFMO were injected into hSGLT1-expressing oocytes and hSGLT1-mediated AMG uptake was measured 1 h later. (B) Downregulation of hSGLT1 by hRS1-Reg is blunted by 1 μM putrescine. hRS1-Reg or hRS1-Reg plus putrescine were injected into hSGLT1-expressing oocytes and hSGLT1-mediated AMG uptake was measured after 1 h. (C) hCNT1-mediated uptake of uridine is downregulated by hRS1-Reg, but not by DFMO inhibition of endogeneous ODC activity. hRS1-Reg or DFMO was injected into hCNT1-expressing oocytes and hCNT1-mediated uridine uptake was measured after 1 h. Mean values ± SE of 25-30 oocytes from three independent experiments are shown. ***$P < 0.001$ ANOVA with post hoc Tukey comparison.

Fig. 8. DFMO and hRS1-Reg downregulate D-glucose-induced short-circuit currents and plasma membrane abundance of hSGLT1 in oocytes expressing hSGLT1-YFP. hSGLT1-YFP was expressed in oocytes by cRNA injection and 3 days incubation. 3 mM DFMO, 1 μM hRS1-Reg(S20E) or 3 mM DFMO plus 1 μM hRS1-Reg(S20E) were injected. One hour later short-circuit currents at -50 mV were measured that were induced by a saturating D-glucose concentration of 100 mM (A) or YFP fluorescence associated with the plasma membrane of the oocytes was analyzed (B,C). Typical fluorescence pictures (B) or densitrometric quantification of plasma membrane-associated YFP fluorescence is shown (C). Mean values ± SE of 7-10 oocytes derived from two independent experiments are shown. ***$P < 0.001$ for difference to oocytes without injection of compounds, ANOVA with post hoc Tukey comparison.

Fig. 9. Non-additive downregulation of phorizin-inhibited AMG uptake in Caco-2 cell by DFMO and hRS1-Reg. Caco-2 cells that had been cultivated for 18 days in medium containing 1 mM D-glucose were incubated for 30 min at 37^{o}C with medium, medium containing unloaded nanohydrogel (gel), medium containing hRS1-Reg(S20E) linked to nanohydrogel (gel-hRS1-RS1-Reg(S20E), medium

Molecular Pharmacology Fast Forward. Published on August 23, 2016 as DOI: 10.1124/mol.116.104521
This article has not been copyedited and formatted. The final version may differ from this version.

with 5 mM DFMO or medium containing gel-hRS1-RS1-Reg(S20E) plus DFMO. After washing the monolayers were incubated for 10 min (37^{o}C) in the presence of sodium with 0.7 μM [^{14}C]AMG in the absence of phlorizin or in presence of 1mM phlorizin. Phlorizin-inhibited uptake was calculated. Mean values ± SD from six measurements performed in two independent experiments are shown. ***$P < 0.001$ for difference to medium control, ANOVA with post hoc Tukey comparison.

Fig. 10. Proposed mechanism for the interactions of RS1 and D-glucose on ODC-stimulated release of SGLT1-containing vesicles from the TGN. ODC-mediated generation of putrescine stimulates the release of vesicle containing SGLT1 from TGN. Binding of RS1 via its activated RS1-Reg domain inhibits enzymatic activity of ODC which leads to downregulation of vesicle release. Binding of glucose to ODC induces a conformational change that decreases the efficacy for inhibition of ODC activity in response to RS1-Reg binding. This leads to a relief of ODC-mediated vesicle release. RS1-Reg with a phosphorylation pattern that binds to ODC1 and induces a conformational change leading to inhibition of enzymatic activity, and the RS1-Reg binding site of ODC are indicated in blue. D-glucose and the glucose binding site of ODC1 are indicated in red.

Molecular Pharmacology Fast Forward. Published on August 23, 2016 as DOI: 10.1124/mol.116.104521
This article has not been copyedited and formatted. The final version may differ from this version.

Tables

TABLE 1

Kinetic rate and equilibrium binding constant values which were determined by SPR for the interaction of hRS1-Reg(S20A) and hRS1-Reg(S20E) with immobilized hODC1

SPR analysis was performed in the absence and presence of 1 mM D-glucose or after treatment of the flow channel with 1 mM DFMO. Mean values ± SD from 3 independent experiments are shown. The differences between hRS1-Reg(S20A) and hRS1-Reg(S20E), hRS1-Reg(S20E) and hRS1-Reg(S20E) with 1 mM D-glucose, and hRS1-Reg(S20E) and hRS1-Reg(S20E) with 1 mM DFMO are not statistically significant.

	k_{on} [$\times 10^4$ $M^{-1}s^{-1}$]	k_{off} [$\times 10^{-3}$ s^{-1}]	K_D[nM]
hRS1-Reg(S20A)	0.9 ± 0.2	0.6 ± 0.1	68 ± 20
hRS1-Reg(S20E)	0.8 ± 0.3	0.9 ± 0.4	102 ± 25
hRS1-Reg(S20E) with 1 mM D-glucose	0.5 ± 0.1	0.7 ± 0.1	161 ± 35
hRS1-Reg(S20A) with 1 mM DMFO	0.9 ± 0.7	0.6 ± 0.4	85 ± 12

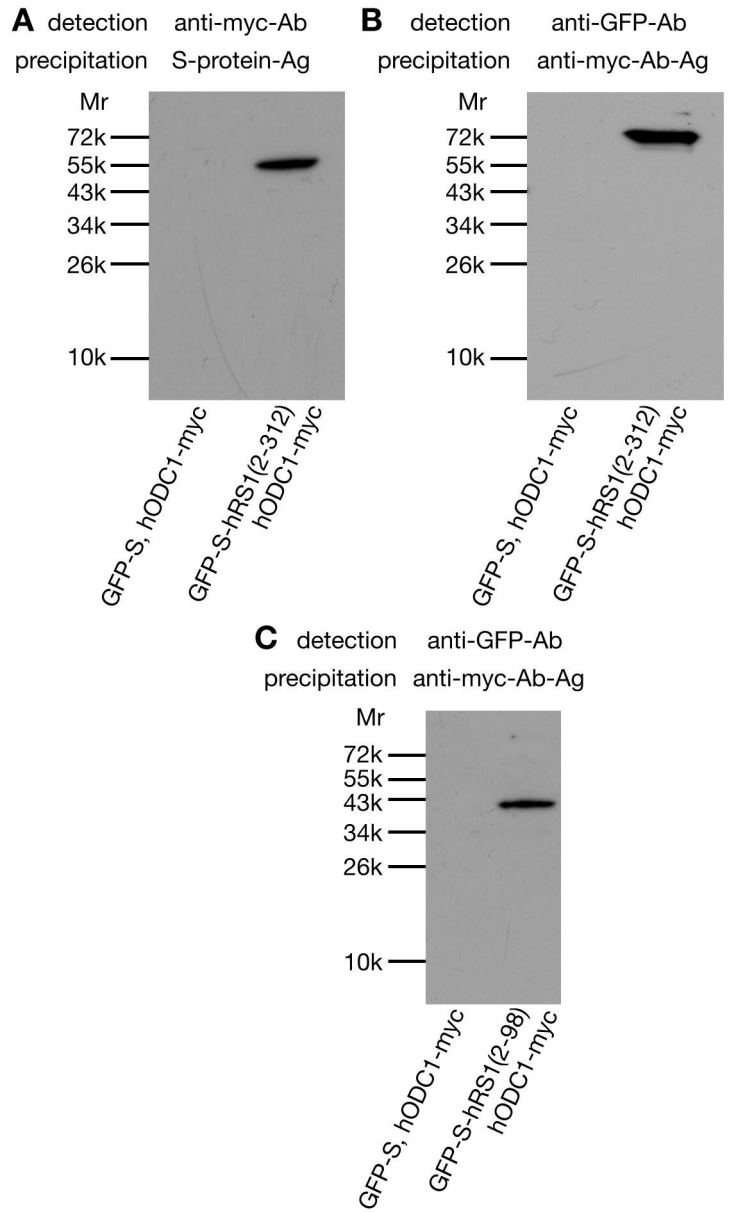
A detection anti-myc-Ab
precipitation S-protein-Ag
Mr
72k
55k
43k
34k
26k
10k
GFP-S, hODC1-myc
GFP-S-hRS1(2-312) hODC1-myc
B detection anti-GFP-Ab
precipitation anti-myc-Ab-Ag
Mr
72k
55k
43k
34k
26k
10k
GFP-S, hODC1-myc
GFP-S-hRS1(2-312) hODC1-myc
C detection anti-GFP-Ab
precipitation anti-myc-Ab-Ag
Mr
72k
55k
43k
34k
26k
10k
GFP-S, hODC1-myc
GFP-S-hRS1(2-98) hODC1-myc

Fig. 1.

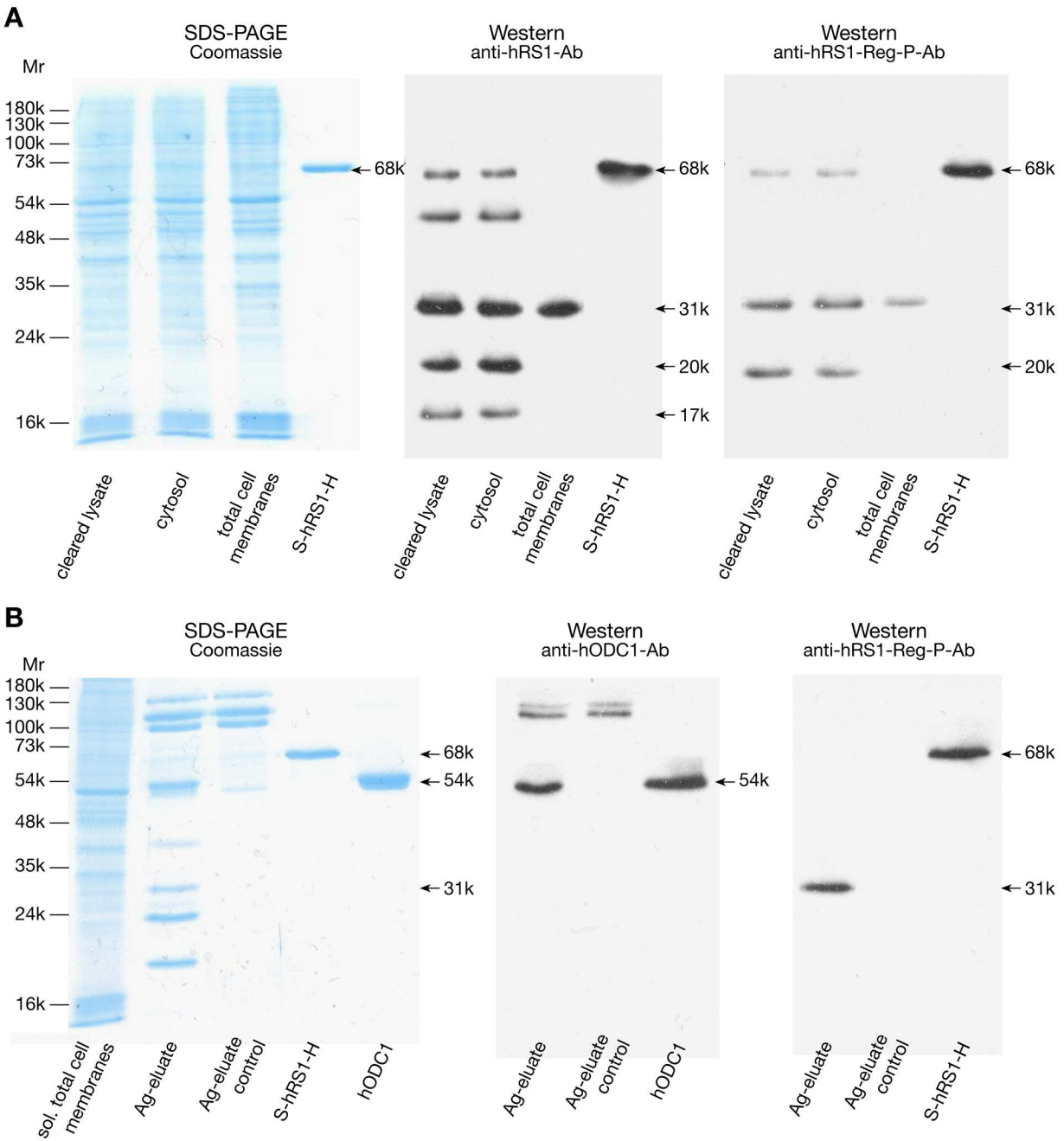
A
SDS-PAGE
Coomassie
Western
anti-hRS1-Ab
Western
anti-hRS1-Reg-P-Ab
Mr
180k
130k
100k
73k
54k
48k
35k
24k
16k
68k
31k
20k
17k
cleared lysate
cytosol
total cell membranes
S-hRS1-H
B
SDS-PAGE
Coomassie
Western
anti-hODC1-Ab
Western
anti-hRS1-Reg-P-Ab
Mr
180k
130k
100k
73k
54k
48k
35k
24k
16k
68k
54k
31k
sol. total cell membranes
Ag-eluate
Ag-eluate control
S-hRS1-H
hODC1

Fig. 2.

Molecular Pharmacology Fast Forward. Published on August 23, 2016 as DOI: 10.1124/mol.116.104521
This article has not been copyedited and formatted. The final version may differ from this version.

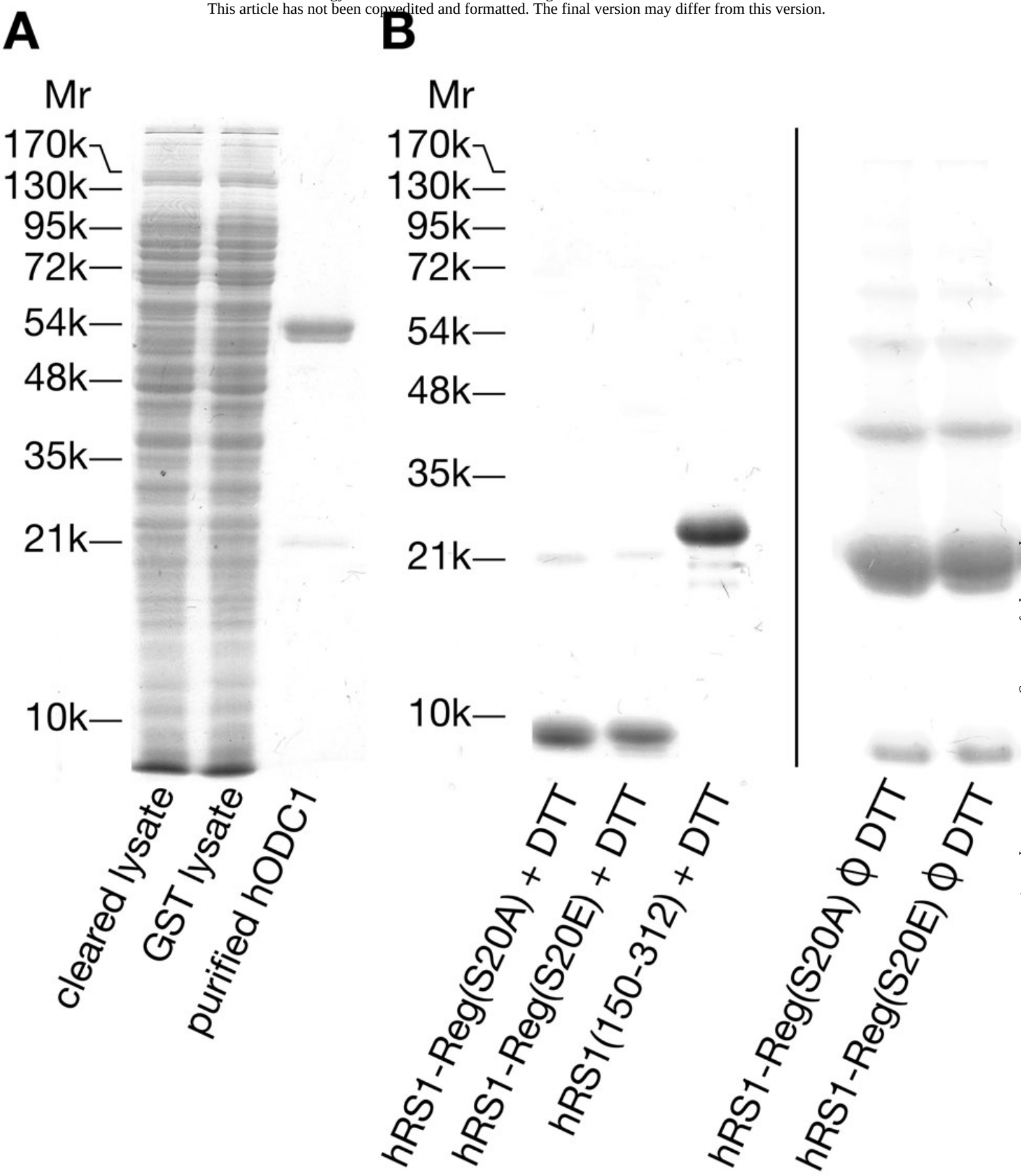

Fig. 3.

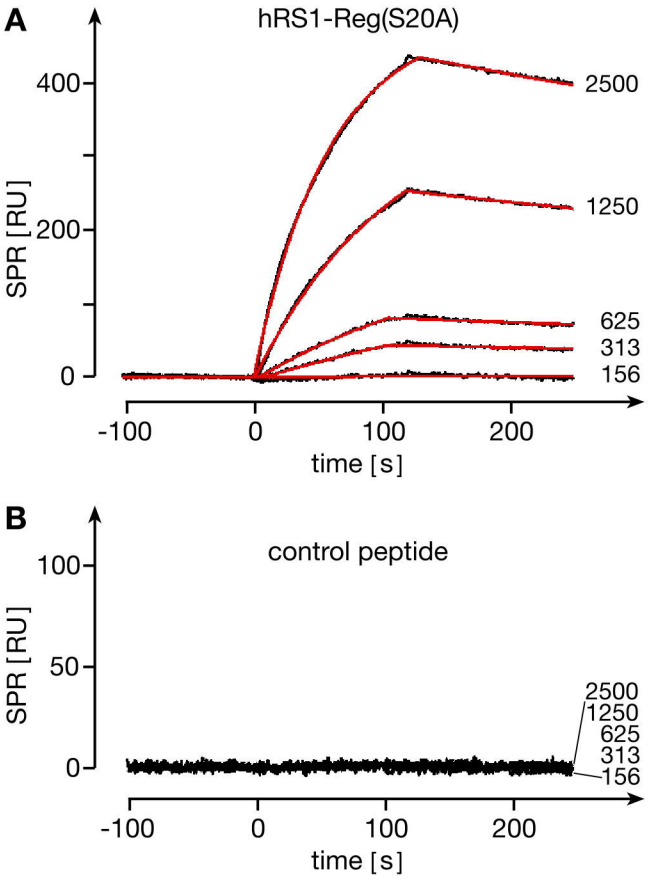
A
hRS1-Reg(S20A)
400
200
0
SPR [RU]
2500
1250
625
313
156
-100
0
100
200
time [s]
B
control peptide
100
50
0
SPR [RU]
2500
1250
625
313
156
-100
0
100
200
time [s]

Fig. 4.

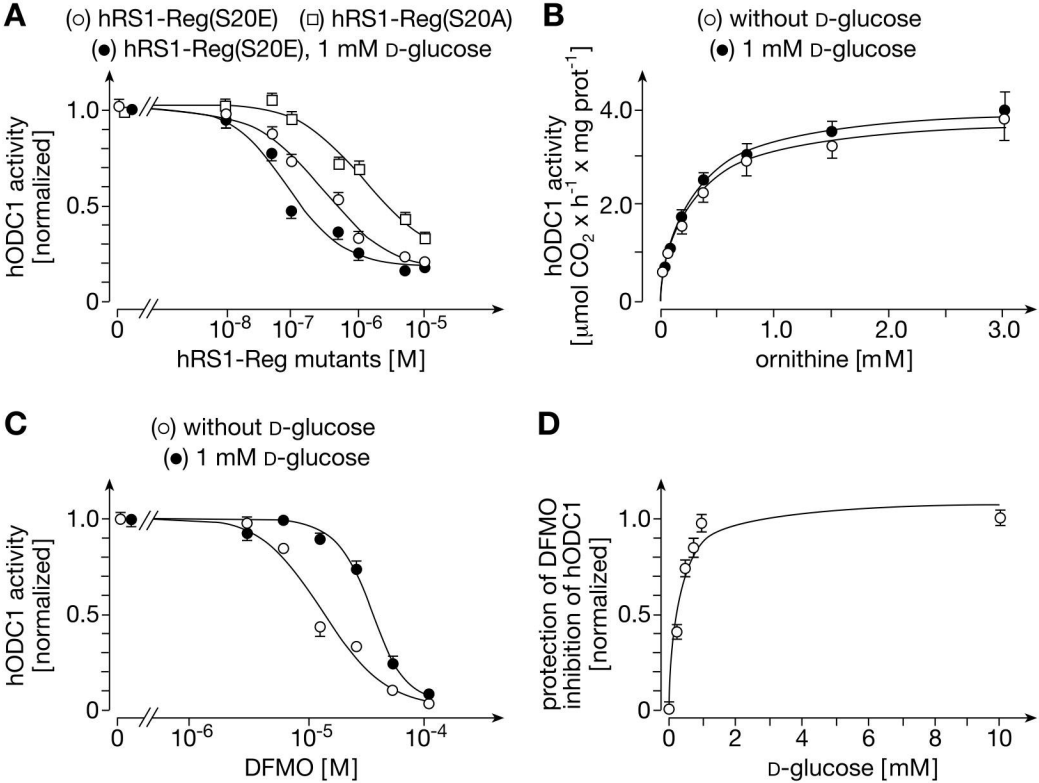
A
(○) hRS1-Reg(S20E) (□) hRS1-Reg(S20A)
(●) hRS1-Reg(S20E), 1 mM D-glucose
hODC1 activity [normalized]
1.0
0.5
0
0
10-8
10-7
10-6
10-5
hRS1-Reg mutants [M]
B
(○) without D-glucose
(●) 1 mM D-glucose
hODC1 activity [µmol CO2 x h-1 x mg prot-1]
4.0
2.0
0
0
1.0
2.0
3.0
ornithine [mM]
C
(○) without D-glucose
(●) 1 mM D-glucose
hODC1 activity [normalized]
1.0
0.5
0
0
10-6
10-5
10-4
DFMO [M]
D
protection of DFMO inhibition of hODC1 [normalized]
1.0
0.5
0
0
2
4
6
8
10
D-glucose [mM]

Fig. 5.

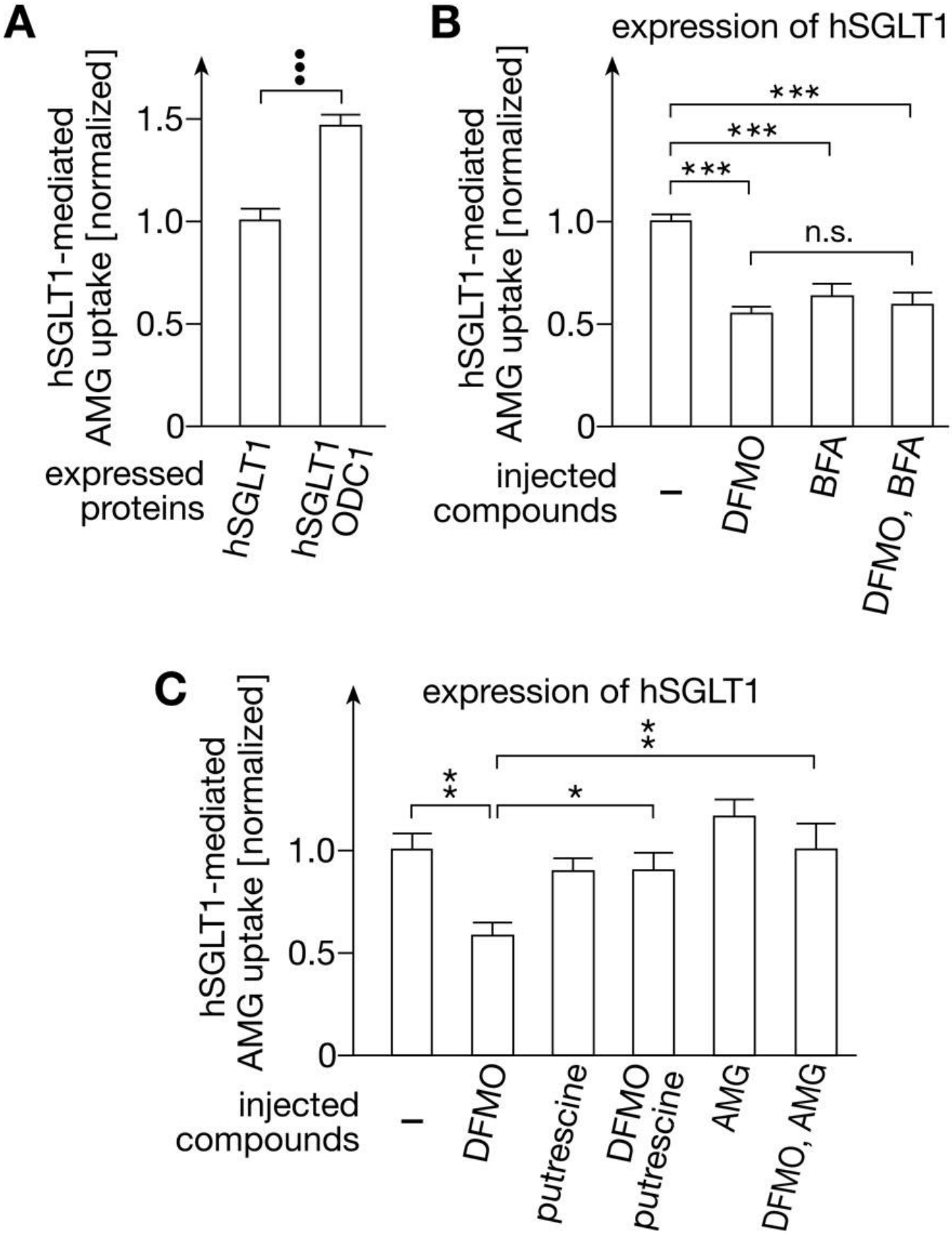
A
hSGLT1-mediated
AMG uptake [normalized]
1.5
1.0
0.5
0
expressed
proteins
hSGLT1
hSGLT1
ODC1
B
expression of hSGLT1
hSGLT1-mediated
AMG uptake [normalized]
***
***
***
n.s.
1.0
0.5
0
injected
compounds
–
DFMO
BFA
DFMO, BFA
C
expression of hSGLT1
hSGLT1-mediated
AMG uptake [normalized]
**
**
*
1.0
0.5
0
injected
compounds
–
DFMO
putrescine
DFMO
putrescine
AMG
DFMO, AMG

Fig. 6.

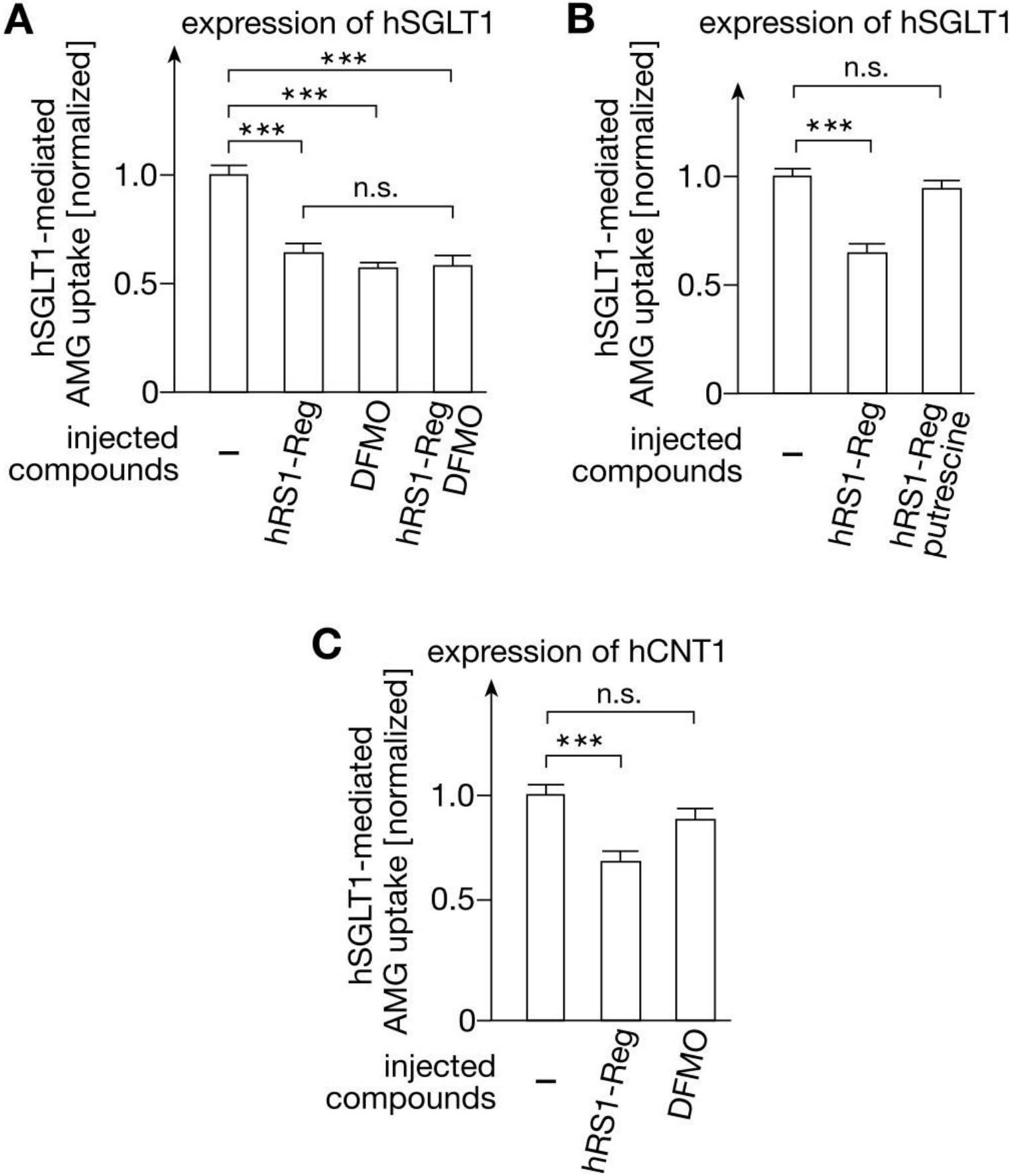
A
expression of hSGLT1
hSGLT1-mediated AMG uptake [normalized]
1.0
0.5
0
***
***
***
n.s.
injected compounds
–
hRS1-Reg
DFMO
hRS1-Reg DFMO
B
expression of hSGLT1
hSGLT1-mediated AMG uptake [normalized]
1.0
0.5
0
n.s.
***
injected compounds
–
hRS1-Reg
hRS1-Reg putrescine
C
expression of hCNT1
hSGLT1-mediated AMG uptake [normalized]
1.0
0.5
0
n.s.
***
injected compounds
–
hRS1-Reg
DFMO

Fig. 7.

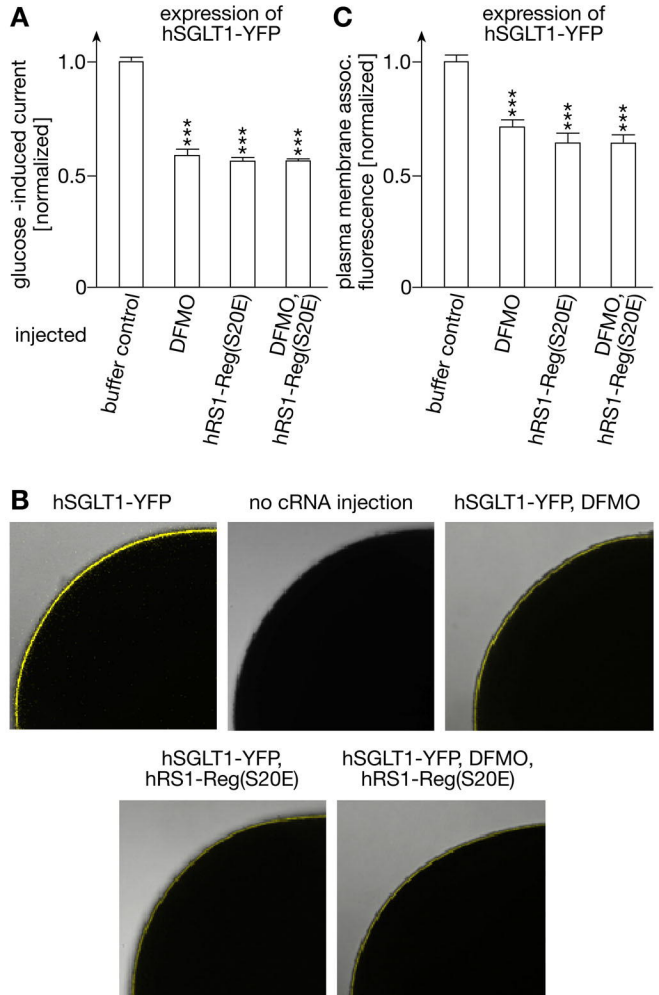
A
expression of hSGLT1-YFP
glucose -induced current [normalized]
1.0
0.5
0
***
***
***
injected
buffer control
DFMO
hRS1-Reg(S20E)
DFMO, hRS1-Reg(S20E)
C
expression of hSGLT1-YFP
plasma membrane assoc. fluorescence [normalized]
1.0
0.5
0
***
***
***
buffer control
DFMO
hRS1-Reg(S20E)
DFMO, hRS1-Reg(S20E)
B
hSGLT1-YFP
no cRNA injection
hSGLT1-YFP, DFMO
hSGLT1-YFP, hRS1-Reg(S20E)
hSGLT1-YFP, DFMO, hRS1-Reg(S20E)

Fig. 8.

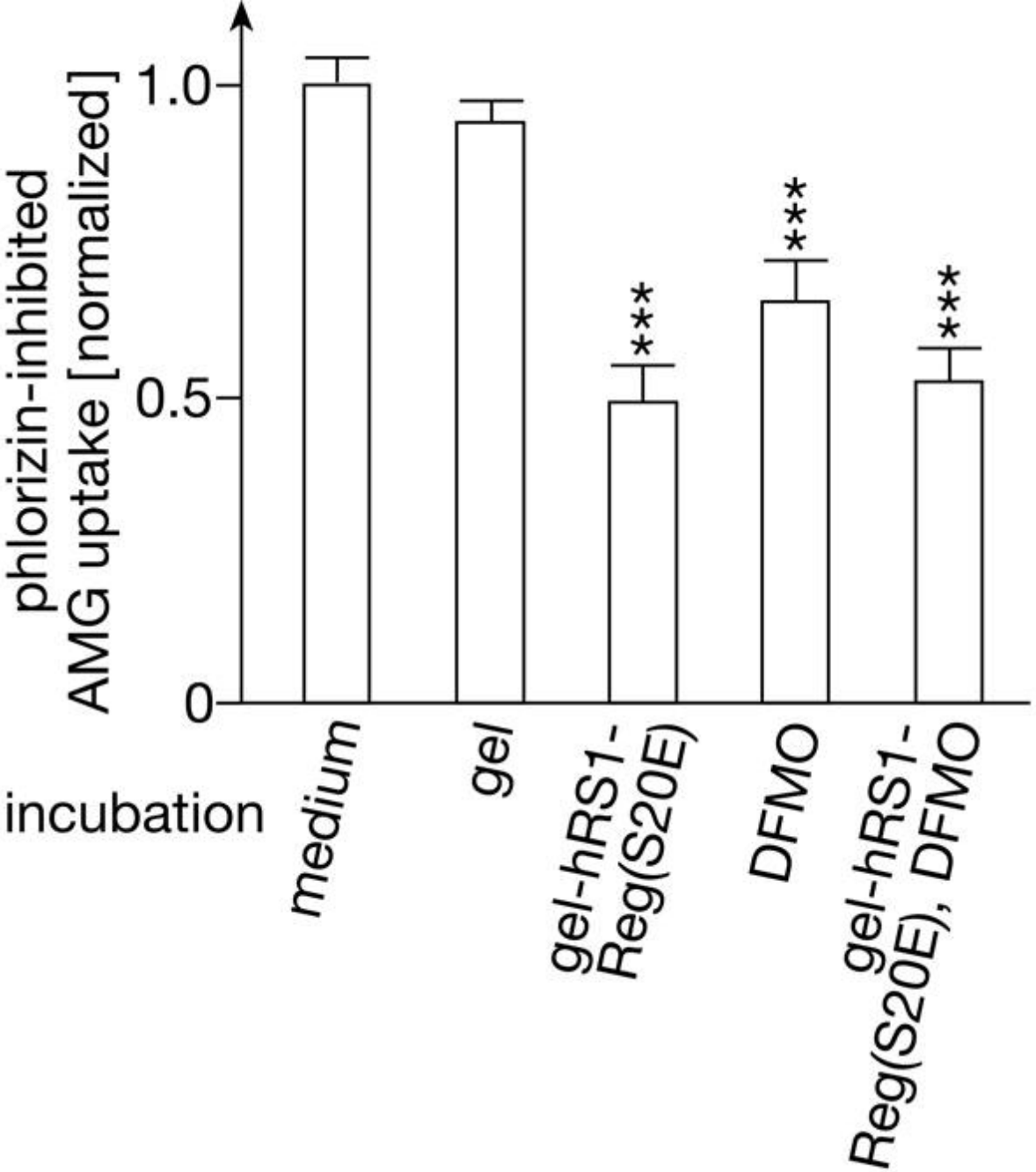
phlorizin-inhibited
AMG uptake [normalized]
1.0
0.5
0
***
***
***
incubation
medium
gel
gel-hRS1-Reg(S20E)
DFMO
gel-hRS1-Reg(S20E), DFMO

Fig. 9.

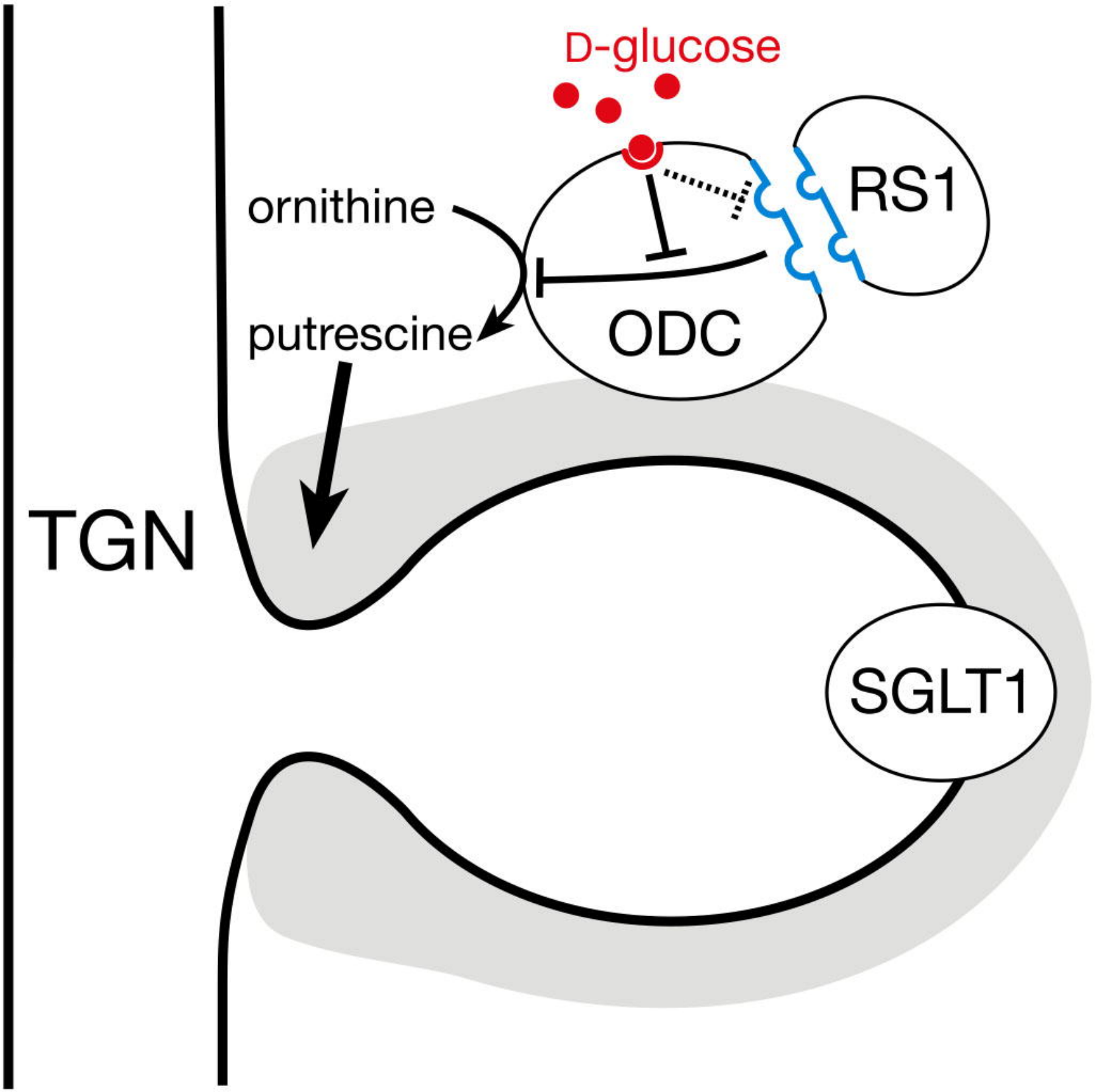

Fig. 10.